FOLOU
D3.2 – Report on testing results of all the FOLOU Innovative solutions

Author(s):	*Wouter Maes, UGent* *Driss En-Nejjary, UGent;* *Contributions by partners from CIRCE, Dilepix, UniVPM*
Version:	*Final version*
Quality review:	*Nancy Peña, UVIC* *Anna Sagrera UVIC*
Date:	*22/12/2025*
Dissemination level:	*Public (PU)*
Grant Agreement N°:	*101084106*
Starting Date:	*01/01/2023*
Duration:	*48 months*
Coordinator:	*UVIC*
Contact details:	*wouter.maes@ugent.be*

Funded by the European Union. Views and opinions expressed are however those of the author(s) only and do not necessarily reflect those of the European Union or the European Research Executive Agency (REA). Neither the European Union nor the granting authority can be held responsible for them.

Document history

Version	Date	Author	Description of change
V1	04/07/2025	Wouter Maes Driss EN-NEJJARY	Draft version of the structure
V2	18/072025	Wouter Maes Driss EN-NEJJARY	Final structure+ T3.2 section as an example
V3	28/11/2025	UGENT, UNIVPM, Dilepix, CIRCE	Third draft version with input from all task leaders
V4	15/12/2025	UGENT, UNIVPM, Dilepix, CIRCE	Revised version with input from partners and external reviewers
VF	22/12/2025	Wouter Maes	Final version approved
VF rev	08/05/2026	UGENT, UNIVPM, Dilepix, CIRCE, UVIC	Final version approved and revised after the review meeting

Funded by the European Union. Views and opinions expressed are however those of the author(s) only and do not necessarily reflect those of the European Union or the European Research Executive Agency (REA). Neither the European Union nor the granting authority can be held responsible for them.

Table of Contents

Funded by the European Union. Views and opinions expressed are however those of the author(s) only and do not necessarily reflect those of the European Union or the European Research Executive Agency (REA). Neither the European Union nor the granting authority can be held responsible for them.

Funded by the European Union. Views and opinions expressed are however those of the author(s) only and do not necessarily reflect those of the European Union or the European Research Executive Agency (REA). Neither the European Union nor the granting authority can be held responsible for them.

Funded by the European Union. Views and opinions expressed are however those of the author(s) only and do not necessarily reflect those of the European Union or the European Research Executive Agency (REA). Neither the European Union nor the granting authority can be held responsible for them.

List of Figures

Funded by the European Union. Views and opinions expressed are however those of the author(s) only and do not necessarily reflect those of the European Union or the European Research Executive Agency (REA). Neither the European Union nor the granting authority can be held responsible for them.

Funded by the European Union. Views and opinions expressed are however those of the author(s) only and do not necessarily reflect those of the European Union or the European Research Executive Agency (REA). Neither the European Union nor the granting authority can be held responsible for them.

List of Tables

Funded by the European Union. Views and opinions expressed are however those of the author(s) only and do not necessarily reflect those of the European Union or the European Research Executive Agency (REA). Neither the European Union nor the granting authority can be held responsible for them.

Abbreviations

Abbreviation	Meaning
BAU	Business As Usual
BBCH	Biologische Bundesanstalt, Bundessortenamt und CHemische Industrie
CV	Coefficient of Variation
DSSAT	Decision Support System for Agrotechnology Transfer
DSTAT	D-statistic
ECV	Enhanced Conventional
ES	Exponential Smoothing
FL	Food Loss
GSD	Ground Sampling Distance
LAI	Leaf Area Index
LR	Linear Regression
MAE	Mean Absolute Error
MLP	MultiLayer Perceptron
NIR	Near Infrared
PCC	Pearson Correlation Coefficient
RGB	Red Green Blue
RMSE	Root Mean Square Error
SPAD	Soil Plant Analysis Development
SSP	Shared Socioeconomic Pathways
SVM	Support Vector Machines
UNILET	French national association for canned and frozen vegetables
VIS	Visible
WP	Work Package
ZST	Zero-Stress

Funded by the European Union. Views and opinions expressed are however those of the author(s) only and do not necessarily reflect those of the European Union or the European Research Executive Agency (REA). Neither the European Union nor the granting authority can be held responsible for them.

Glossary

Annotation: Human-performed classification, localization or detection.

Bounding box: Rectangle with the smallest area containing all pixels belonging to an object, with sides parallel to image edges.

Coefficient of variation: Statistical measure of variability or inequality within a dataset, defined as the ratio of the standard deviation to the mean.

Detection neural network: A deep learning model designed to identify and localize objects within an image or video.

Funded by the European Union. Views and opinions expressed are however those of the author(s) only and do not necessarily reflect those of the European Union or the European Research Executive Agency (REA). Neither the European Union nor the granting authority can be held responsible for them.

Executive Summary

This document reports on the first results of WP3 of the FOLOU project. This WP focuses on technological solutions for food loss measurements. It builds upon Deliverable D3.1, which addressed the design, technical description and development of the different technological solutions. The current deliverable D3.2 consists of a technical report of the tested innovative solutions, including the main results of the testing and validation phases, the accuracy of the developed method, and the monitoring plan to ensure obtention of optimal quantification/estimation. The initial testing phase confirmed that each task is on the right path, showing their feasibility and promising potential performance of the proposed solutions.

Following the previous structure, the document is organized into distinct cases, each targeting specific types of food losses and commodities:

1. Tractor-embedded video cameras for assessing food loss in vegetable crops (Dilepix-T3.1)
2. UAV-based high-resolution RGB for food loss assessment in apple (UGent-T3.2)
3. Repeated multispectral and satellite data for production loss assessment in potato, maize, corn, faba bean and sunflower (Uni-VPM and UGent, T3.2 & T3.3)
4. Automated fish egg sorting using multispectral camera technology in trout aquaculture (UNIVPM-T3.4)
5. Blockchain technology implementation in mussel aquaculture (UNIVPM-T3.5)
6. Market demand tools from social networks (CIRCE-T3.6)

Deliverable D3.2 reports the outcomes of the initial testing phase of all innovations and provides an overview of the progress of the work realized by all partners contributing to WP3. The first results confirm the soundness of the proposed approaches and provide a solid foundation for the upcoming large-scale validation activities under WP4.

Together, these advancements demonstrate that WP3 has progressed from prototype development to early validation, showing measurable progress toward FOLOU's objectives of quantifying.

Funded by the European Union. Views and opinions expressed are however those of the author(s) only and do not necessarily reflect those of the European Union or the European Research Executive Agency (REA). Neither the European Union nor the granting authority can be held responsible for them.

Introduction

The purpose of WP3 is to develop technological tools to measure and estimate food losses at the primary production stage across various agricultural sectors, including vegetables, fruits, and horticultural crops leveraging the revolutionary advancements in remote proxy sensing, as well as the cutting-edge capabilities of AI. The final goal is to develop methods that could partially replace the time-consuming and expensive manual sampling needed today to quantify food losses in the primary sector.

This deliverable reports the testing results of all the FOLOU innovative solutions and shows the technical feasibility and initial performance metrics of each solution, confirming their readiness to move to the next stage of validation (TRL) and deployment within the FOLOU framework.

This report is a direct follow-up to Deliverable *D3.1*: *Technical description of all the FOLOU Innovative solutions developed* that provided the comprehensive technical specifications, planned methodologies, data acquisition protocols, and the theoretical framework for each solution.

D3.2 now provides the new activities and report the results of the initial tests, the performance metrics achieved. The structure of this deliverable follows the logical progress of the work conducted within WP3, with an overview given of the technical development per task:

1. **Task 3.1:** Validation of computer vision and deep learning solutions for food loss detection in vegetable crops using tractor-mounted and drone-based imaging.
2. **Task 3.2:** UAV-based RGB imaging for quantifying food losses in fruit orchards, focusing on apple and orange case studies.
3. **Task 3.3:** Application of multispectral and satellite data, combined with crop modelling, for assessing production losses in major field crops.
4. **Task 3.4:** Development and validation of an automated system for monitoring trout embryos using multispectral imaging and AI.
5. **Task 3.5:** Implementation of a blockchain-based digital platform ensuring data integrity and traceability in aquaculture.
6. **Task 3.6:** Development of AI-based tools that use social network and search engine data to anticipate consumption trends and assess potential food loss scenarios.

As showed above, not all of the technological solutions under development in WP3 cover all categories of food losses, as well as there are some that focus on Production losses rather than on Food losses. These specifications have been also agreed and aligned with the activities under WP4.

The document concludes with a Summary and Conclusions section, which synthesizes the key progress and outcomes of the initial results.

Funded by the European Union. Views and opinions expressed are however those of the author(s) only and do not necessarily reflect those of the European Union or the European Research Executive Agency (REA). Neither the European Union nor the granting authority can be held responsible for them.

1. Tractor-embedded video cameras for assessing food loss in vegetable crops (Dilepix-T3.1)

1.1 Overview

The aim of this task is to explore the use of RGB video cameras mounted on tractors and drones flying at low altitude combined with Deep Learning and Computer Vision algorithms to detect and localize food losses in vegetable crops.

As mentioned in D3.1, the use of drones was considered due to difficulties related to logistics and tractor manoeuvrability in the field. The task focuses on developing algorithms, testing the solution, and validating it at regional and national levels to provide a more efficient alternative to traditional, costly, and time-consuming manual measurement methods.

To support these activities, several data acquisition campaigns were carried out in cauliflower and lettuce plots during each subperiod of the task. These datasets were essential for the development of algorithms, their testing, and the subsequent validation of the solution.

Timeline (M01–M42):

- M01–M24: Development of the solution and algorithms, supported by initial data acquisition campaigns in France
- M13–M24: Testing of the solution, using datasets collected in field trials in Spain
- M25–M42: Validation in France and the Catalan region, with additional data acquisition to refine and confirm results

1.2 Material & Methods

1.2.1. Data Acquisition Strategy

The acquisition strategy of Task 3.1 was designed to ensure replicability of the developed solution across different regions and crops. Initially, available crops in France and Spain were listed, with growing and harvesting calendars established to guide data collection. Following the first feedback on the Food Loss Definition Framework in summer 2023, cauliflower was selected as the first focus crop, as its harvest period (October–November) matched the project's timeline and it was common to both France and Spain.

With the support of Unilet, Dilepix carried out the first data acquisition campaigns in cauliflower fields in Brittany (France). In the subsequent phases, new datasets were acquired in Catalonia (Spain, extending the scope to both cauliflower and lettuce to support testing and validation of the solution (See Figure 1.1).

Funded by the European Union. Views and opinions expressed are however those of the author(s) only and do not necessarily reflect those of the European Union or the European Research Executive Agency (REA). Neither the European Union nor the granting authority can be held responsible for them.

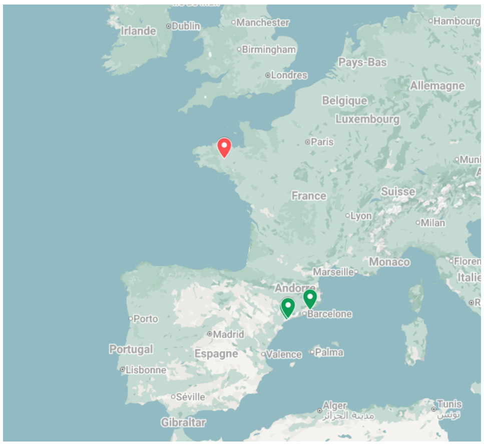

Figure 1.1 List of acquisition areas (Red: M0-M12; Green: M13-M24)

Data acquisition has been performed at different maturity stages:

- Pre-harvesting (about 2 to 3 weeks before harvesting).
- During harvesting (As the harvesting of these crops is undertaken multiple times, this results in acquisitions of partially harvested fields).
- Post-harvesting.

Moreover, this strategy has been completed with manual annotations from the measurements of WP4 case studies. This way, the data contrasted and the models are finetuned in order to improve the detection of the images.

1.2.2. Material and Equipment

Task 3.1 focuses on RGB video cameras embedded on tractors. However, bringing a tractor into a field can become complex as the cultivation process advances. The growth of crops alters the terrain, leading to uneven surfaces, obstacles, and narrower pathways, which can challenge tractor manoeuvrability. Additionally, the presence of delicate crops or intricate planting arrangements demands precision and care to avoid damage. Moreover, environmental factors such as weather conditions and soil moisture levels further complicate tractor operation, requiring adjustments in approach and timing.

For these reasons and to make sure data can be acquired all over the FOLOU project, it was decided to **simulate** initial embedded cameras on the tractor by **using a drone flying low altitude.** The processing pipeline is summarized in Figure 1.2; Figure 1.3 illustrates the data capture process with images.

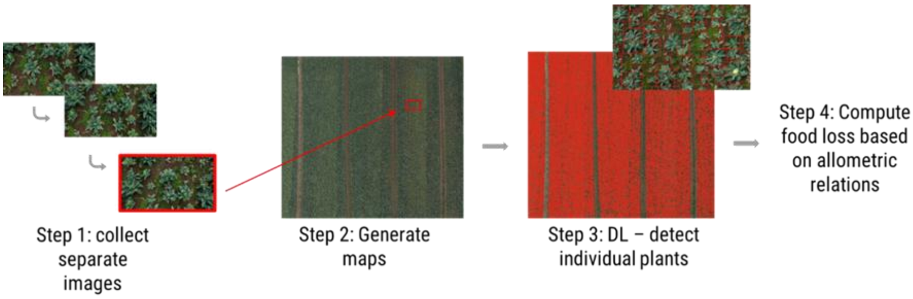

Figure 1.2. Current software pipeline

Funded by the European Union. Views and opinions expressed are however those of the author(s) only and do not necessarily reflect those of the European Union or the European Research Executive Agency (REA). Neither the European Union nor the granting authority can be held responsible for them.

Figure 1.3. DJI Mavic Pro 2 UAV flying over cauliflower field (top); Flight planning through DJIFlightPlanner and Litchi Mission Hub (bottom).

1.2.3. Collected Data

In 2023 (M0 – M12), thanks to a valuable collaboration with farmers in Brittany, France, the Dilepix team gained repeated access to cauliflower fields. This allowed us to collect extensive data, resulting in:

- Over 60 drone-captured videos.
- Approximately 100 complementary images.
- An additional 150 images and 40 videos captured using supplementary equipment (smartphones, GoPro cameras, etc.), primarily for communication and internal learning purposes.

These datasets were initially used to develop the solution of T3.1 and described in D3.1.

Funded by the European Union. Views and opinions expressed are however those of the author(s) only and do not necessarily reflect those of the European Union or the European Research Executive Agency (REA). Neither the European Union nor the granting authority can be held responsible for them.

Figure 1.4 Images extracted from video acquired in 2023.

Figure 1.5 Images extracted from video acquired in 2024.

Figure 1.6 Manual food loss quantification & data acquisition with low altitude drone.

Funded by the European Union. Views and opinions expressed are however those of the author(s) only and do not necessarily reflect those of the European Union or the European Research Executive Agency (REA). Neither the European Union nor the granting authority can be held responsible for them.

In 2024 (M13 – M24), new data acquisitions were carried out in Spain (Mataró, Reus, and Tarragona) in collaboration with ESPIGOL (WP4) to test and validate the methodology in comparison to manual measurements. This resulted in:

- Around 20 drone-captured videos.
- Manual food loss quantification conducted as ground truth.
- Data collected across multiple cauliflower and lettuce fields.

The model was further tested with different crops (lettuces) and territory to analyse its performance and extract other metrics. But especially, this comparison was useful in order to obtain more data and finetune the model.

1.2.4. Data preparation

Acquired datasets from both years 2023 and 2024 have been fully annotated and processed using the pipeline detailed in D3.1 for data annotation and augmentation. The data were collected at fields very shortly before the actual harvest, thus representing a good starting point to measure food losses.

As a result of data preparation, in 2023 (M0 – M12):

- A total of **4199** individual cauliflowers were annotated, of which were used for training, validating and testing the neural network model. Individual cauliflowers used for validation have been randomly selected from the training dataset and a total of 661 were kept for evaluation.
- Data augmentation has been performed leading to **18592** augmented cauliflower targets.

In 2024 (M13–M24), **1350 new units** were annotated from cauliflower and lettuce fields. These annotations were not used for neural network training but served as a basis for extracting other metrics including weight estimates, which were then compared to manual food loss quantifications, as is specified below (see Section 2.3 – "Method Development Activities").

New data acquisition sessions are planned for the end of 2025 and the beginning of 2026 to separate the validation dataset from the training dataset and to further expand the testing dataset.

1.2.5. Method development activities

The software development strategy remains the same as the one detailed in the previous deliverable D3.1 section 1.5 ("The proposed method"), based on modularity.

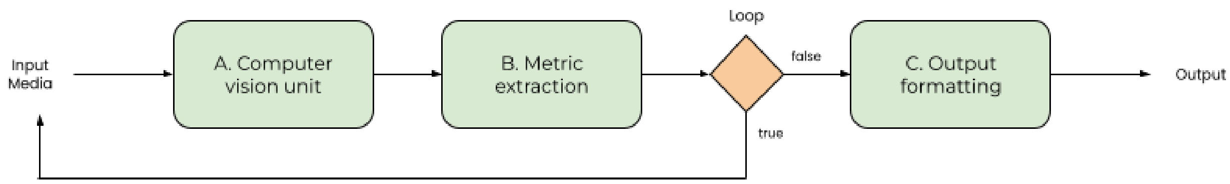

Figure 1.7 Synthetic view of the software architecture of Task 3.1.

Funded by the European Union. Views and opinions expressed are however those of the author(s) only and do not necessarily reflect those of the European Union or the European Research Executive Agency (REA). Neither the European Union nor the granting authority can be held responsible for them.

Figure 1.7 shows a synthetic view of the software architecture. Module A is dedicated to image analysis, relying on deep learning (neural networks). Module B is dedicated to metric extraction, aiming to link generic approaches from Module A to the specific application of FOLOU regarding food loss. Module A and B can then be treated either individually (per image), or globally (based on an orthomosaic of the entire field). By considering individual input, it will provide precise feedback on one specific part of the field. On the other hand, working globally might provide information at the scale of an entire plot or geographical area. Finally, computed metrics can be formatted in Module C to best suit end-user needs.

Following this, an incremental development strategy was adopted divided into two phases:

1. (M0 – M12) Assist manual or direct food loss measurements by providing information on the **field homogeneity**.
2. (M13 – M24) Replace manual or direct food loss measurement with a fully **autonomous solution**.

1.3 First Results

1.3.1. Field homogeneity

To assist manual or direct food loss measurements, we have first decided to specifically tackle the problem of **sampling**. Due to resource limitations, it is not feasible to manually measure an entire plot for its high complexity and cost due to the crop type. The FOLOU Quantification Framework provides guidelines for sampling when doing manual measurements. It includes information on percentage of the plot to consider and recommendations regarding the crop types and terrain characteristics. However, every crop field is different, and those generic guidelines might not be sufficient to get a precise quantification of food loss.

In the metric extraction module, the first step was to exploit the outputs on the computer vision unit e.g. the bounding boxes to measure the homogeneity of the plot – we here refer to the variation in size of the cauliflower within an area, rather than variation in plant density. Each box size of every image of the plot is used to compute a variation coefficient. The coefficient of variation (CV) is a statistical measurement of the degree of variability or inequality within a data series. It is defined as the ratio of the standard deviation σ to the mean μ: $CV = \sigma/\mu$.

The coefficient of variation can be used to get a global view on an entire plot. The output format is a numerical value expressed in percent.

Figure 1.8 Estimation of the homogeneity of a healthy field. Individual cauliflower detections (left) Homogeneity [Variation coefficient=33%] (right).

Funded by the European Union. Views and opinions expressed are however those of the author(s) only and do not necessarily reflect those of the European Union or the European Research Executive Agency (REA). Neither the European Union nor the granting authority can be held responsible for them.

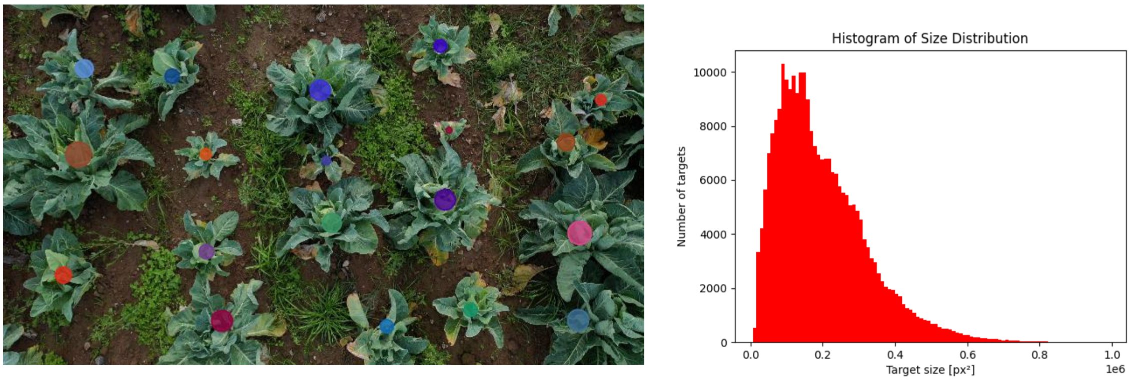

Figure 1.9 Estimation of the homogeneity of a non-healthy field (clubroot disease). Individual cauliflower detections (left) Homogeneity [Variation coefficient=63%] (right).

A healthy field (Figure 1.8) has a more homogenous distribution of sizes than a disease-infected field (Figure 1.9). In this example, the coefficient of variation is 33% against 63% for a non-healthy field, as illustrated visually in the histograms.

While the coefficient of variation (CV) provides a quantitative measure of heterogeneity, effective sampling in a field requires more than a single aggregated metric. By generating spatial maps of CV or size disparity, numerical variability is translated into a visual, field-level representation. (Figure 1.10. Such cartography helps identify zones of high and low variability, localized clusters of small or large vegetables, and transitional areas where conditions change.

This information can directly support the selection of sampling locations for food-loss measurements. Instead of relying on uniform or random sampling, we can intentionally target:

- **Representative zones** (average conditions),
- **Extremes** (areas with particularly high or low CV, Figure 1.11)
- **Transition zones** (where variability shifts).

Targeting these zones ensures that manual food-loss quantification captures the true distribution of remaining vegetables, reduces sampling bias, and increases the interpretability and reliability of the measurements. The maps serve as a decision-support tool that complements, rather than replaces, expert judgement by providing a structured way to prioritize and justify sampling points.

One practical way to operationalize this could be through a stratified sampling approach. Based on the cartography, the field can be divided into several strata reflecting different variability conditions—for example, representative, extreme, and transitional zones. Samples can then be collected within each stratum, either proportionally to its area or weighted by its level of variability. After estimating food loss separately for each zone, the results can be integrated into a field-level estimate by weighting zones according to their relative area. This approach ensures that the main spatial patterns are captured and helps reduce the risk of sampling bias. Future work will integrate this into a scientific sampling strategy, taking within-field variation into account.

Funded by the European Union. Views and opinions expressed are however those of the author(s) only and do not necessarily reflect those of the European Union or the European Research Executive Agency (REA). Neither the European Union nor the granting authority can be held responsible for them.

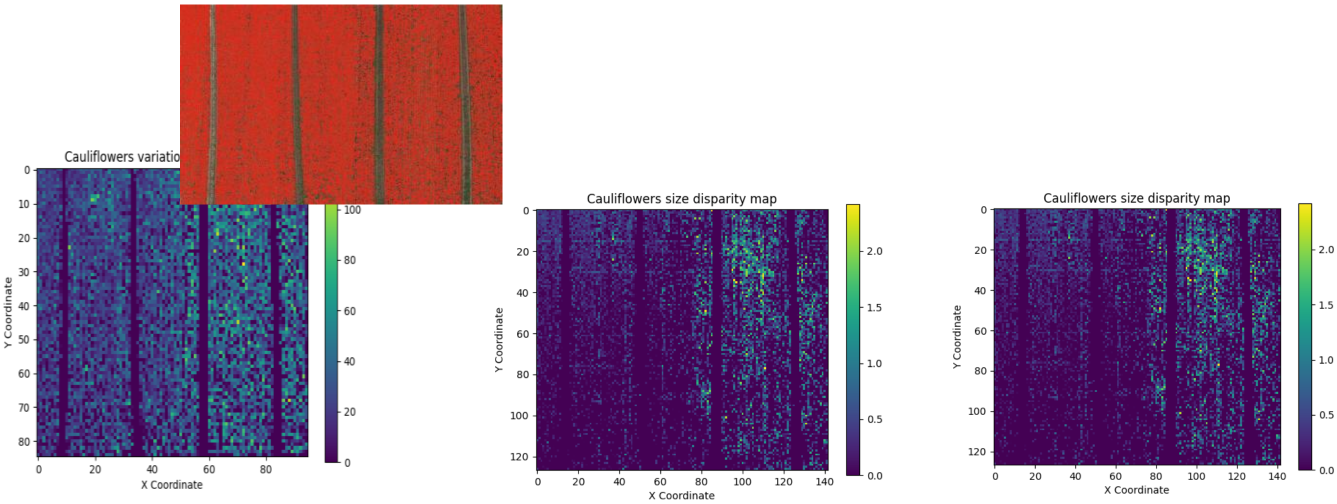

Figure 1.10 Representation of the field with all frames detections (left), computed size disparity map (middle), computed variation coefficient map (right).

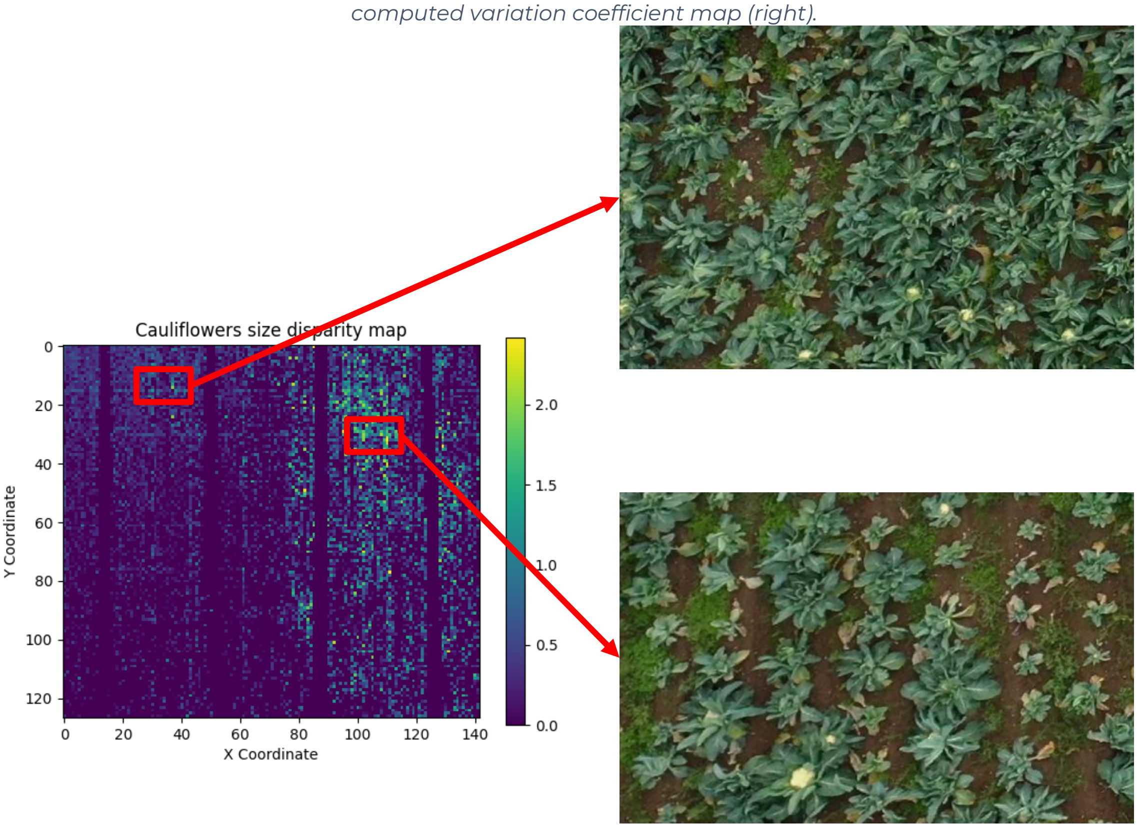

Figure 1.11 Extraction of non-homogeneous areas that should be targeted for manual quantifications.

1.3.2. Autonomous food loss quantification

Measuring food loss directly in the field is an important first step toward effective and more straightforward quantification. However, existing manual protocols are labour-intensive, time-consuming, and limited to sampling only a portion of the field. As a result, the frequency, scale, and precision of data collection remain restricted. An autonomous software solution addresses these challenges by delivering rapid, large-scale, and objective measurements across entire fields. For this reason, developing such a solution became the team main focus in 2024 (M13 – M24) within our software development strategy.

Funded by the European Union. Views and opinions expressed are however those of the author(s) only and do not necessarily reflect those of the European Union or the European Research Executive Agency (REA). Neither the European Union nor the granting authority can be held responsible for them.

The measurements are done just after the harvest and are used to **quantify harvest losses** (in this case, the amount (weight) of vegetables not harvested. The objective was to detect vegetables left behind in the field after harvesting (Figures 1.12 to 1.15) and to estimate their corresponding weight. To achieve this, food loss was quantified by calculating the total weight from the sizes of bounding boxes (manually annotated), combined with the known minimum and maximum unit weights for the crop.

These reference weights were obtained through field sampling (Figure 1.1). Finally, several computation strategies were tested to refine and validate the measurement process:

- **Linear**
- **Power**: Emphasizes bigger boxes more. Suited for vegetal content

Figure 1.12 Orthomosaic showing detected remaining lettuces after harvesting

Figure 1.13 Orthomosaic showing detected remaining cabbages after harvesting

Funded by the European Union. Views and opinions expressed are however those of the author(s) only and do not necessarily reflect those of the European Union or the European Research Executive Agency (REA). Neither the European Union nor the granting authority can be held responsible for them.

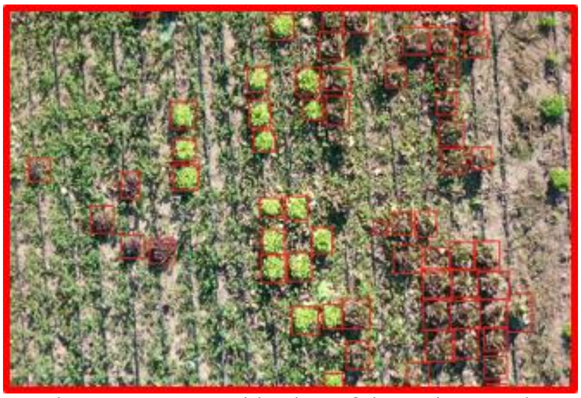

Figure 1.14 Zoomed-in view of the orthomosaic showing detected remaining lettuces after harvesting

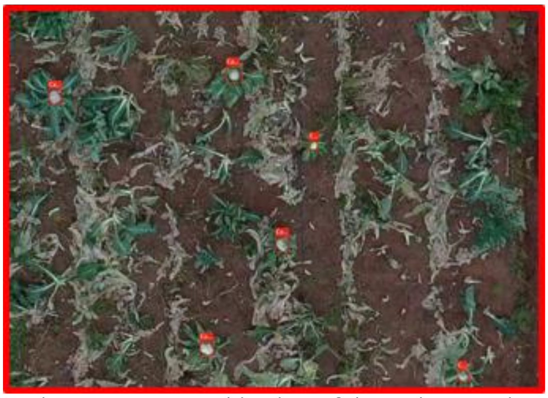

Figure 1.15 Zoomed-in view of the orthomosaic showing detected remaining cauliflowers after harvesting

Figure 1.16 The weight of crops in the field, to be used as reference for crop units.

As a result, it is possible to compare autonomous measurement with manual food loss quantifications. In the tables below are presented two comparisons for lettuce and cauliflower fields (Table 1.1 and 1.2).

Table 1.1 Autonomous food loss quantification on a lettuce field with two weight hypotheses (Manual measurement: 100.5kg).

	Min and max weight of one unit	
	[0.06kg - 0.30kg]	**[0.03kg - 0.60kg]**
Linear	80.41	134.60
Power	64.68	97.26

Table 1.2 Autonomous food loss quantification on a cauliflower field. The manual reference was 379.0 kg.

	Min and max weight of one unit
	[0.50kg - 1.5kg]
Linear	280.06
Power	239.15
Quadratic	218.33
Cubic	200.76
Log	189.00
Exponential	251.82

Funded by the European Union. Views and opinions expressed are however those of the author(s) only and do not necessarily reflect those of the European Union or the European Research Executive Agency (REA). Neither the European Union nor the granting authority can be held responsible for them.

1.4 Discussion

1.4.1 Results vs original goal

Regarding the developed solution, no neural network performance analysis was conducted at this stage, as the number of fields studied was still limited and not representative enough to draw conclusions for a generic solution.

Although there have been advances in the development of a software module that automatically computes the total food loss of a plot by considering the minimum and maximum weight of a unit, the script needs to be further improved. A full analysis with more datasets of the results, comparing measured (reference) and modelled (image-derived) data is also required, and bottlenecks need to be developed.

In the next months, larger-scale data acquisition will be undertaken across more diverse contexts to enable robust evaluation and ensure the solution's adaptability to various conditions and upscaling possibilities.

1.4.2 Key successes and bottlenecks

The software development strategy, based on modularity, allows the solution to be tested incrementally and applied to multiple use cases. Simple metrics, such as the coefficient of variation, can help improve current manual food loss quantification. Additional metrics can also be computed to make this task less complex and less time-consuming.

Importantly, these results demonstrate that autonomous food loss estimation is feasible, with current outputs closely matching manual measurements. This represents a significant step forward in applying innovative solutions, like the one developed in WP3, to the challenge of food loss quantification.

1.4.3 Further steps and planning

Regarding field homogeneity, discussions will be initiated between WP3 and WP4 to explore how this new cartography-based strategy could be incorporated into the manual food-loss quantification protocol. This will probably require a clear demarcation strategy to divide the field into homogeneous areas. The aim would be to define the level of detail required from the spatial maps while ensuring that any proposed approach remains no more complex than the current protocol and is practical and feasible for field implementation.

These discussions could guide pilot testing in selected fields to evaluate how map-guided sampling compares to standard uniform or random sampling, particularly in terms of representativity and reduction of bias.

Based on the outcomes, a refined protocol could be developed, including guidelines for stratified sampling, zone delineation, sample allocation, and integration of zone-specific measurements into field-level estimates. If feasible, dedicated data acquisitions will be planned for 2026 to collect both variability maps and manual food-loss measurements, supporting validation of the approach while keeping the workflow acceptable and doable for field teams.

Funded by the European Union. Views and opinions expressed are however those of the author(s) only and do not necessarily reflect those of the European Union or the European Research Executive Agency (REA). Neither the European Union nor the granting authority can be held responsible for them.

Reaching a truly generic and autonomous solution will require significant effort, as performance depends on capturing the variability of crops, fields, and harvesting conditions. In the coming months, the focus will be on expanding data acquisition through video recording and detailed manual food loss measurements. These measurements will need to be carried out not only on sampled areas but across entire plots, ensuring precise and comprehensive ground-truth data. This step is essential to properly evaluate the developed solution and guide further improvements.

A key aspect of this process is translating computer-vision data into actual food-loss weights is establishing a reliable relationship between the observed size of vegetables in pixels and their real weight. To address this, further actions should include targeted measurements of individual vegetables with precise geolocation, using RTK or similar positioning systems to link physical samples to the spatial maps. Collecting vegetable samples from producers, measuring their size, and weighing them would allow the collection of the data needed to establish accurate size-to-weight relationships. These measurements would enable the development of allometric relationships for each commodity, linking pixel-based size metrics to weight.

1.4.4 Policy recommendations

- Assessing vegetables with high-resolution RGB data, either from drones or tractor-mounted sensors, can yield automated food loss estimates for a relatively low price.
- These assessments should be recommended, as they also provide meaningful insights in (differences in) quality, and as such expand beyond the mere food loss assessment.

Funded by the European Union. Views and opinions expressed are however those of the author(s) only and do not necessarily reflect those of the European Union or the European Research Executive Agency (REA). Neither the European Union nor the granting authority can be held responsible for them.

2. UAV-based high-resolution RGB for food loss assessment in apple (UGent-T3.2)

2.1 Overview

The goal of this task is to provide an accurate estimation of food losses in fruit orchards, using apples and oranges as use cases. To achieve this, a deep learning method using high-resolution RGB imagery data as input has been developed to detect damaged and fallen fruits in orchards (Koirala et al., 2019).

For this purpose, several data acquisition campaigns were conducted to measure pre-harvest and harvest losses in apple and orange orchards, and detection models are being developed and refined.

Timeline (M01–M42):

- M01–M12: Initial UAV and ground-truth data acquisition campaigns in Belgium and France on apple orchards, alongside the development of algorithms for data processing and annotation workflows.
- M13–M24: Model development supported by additional data acquisition campaigns in Spain on orange orchards to improve model generalisation.
- M25–M42: Processing of the orange datasets, further model improvement, and development of multi-view detection methods for loss estimation, followed by final adaptation of the models to the orange use case.

2.2 Materials & Methods

2.2.1 Collected Data

The acquisition protocol followed the methodology established in D3.1 for the apple case study. UAV flights were performed in Jonagold apple orchards using a DJI M350 equipped with a DJI Zenmuse P1 high-resolution RGB camera. Images were acquired close to harvest at approximately 12 m flight altitude. To reduce canopy occlusion and improve fruit visibility, images were collected from different viewing angles, including nadir view at 90° and oblique views at 70° and 50°. For the oblique acquisitions, flights were performed from both sides of the tree rows. Ground truth measurements were collected by sampling trees in each orchard and recording good apples, fallen apples, and damaged apples, together with tree location using RTK GNSS.

Following the same acquisition protocol described in D3.1, the data acquisition campaigns have been ongoing to collect additional datasets for better generalization of the detection models.

In the case of apple, campaigns were carried out in "clean" apple orchards (orchards without apples) conducted in Belgium in two different orchards in May to obtain negative samples which may improve model metrics.

Additionally, to develop a more generalizable fruit detection approach, the dataset was expanded to include oranges. In collaboration with ESPIGOL (WP4), two field campaigns were conducted across 5 plots in Tarragona, Spain: a pre-harvest campaign in March 2025

Funded by the European Union. Views and opinions expressed are however those of the author(s) only and do not necessarily reflect those of the European Union or the European Research Executive Agency (REA). Neither the European Union nor the granting authority can be held responsible for them.

and a post-harvest campaign in June 2025. Working with ESPIGOL allowed the inclusion of other fruit types and obtain manual ground truth measurements for food loss estimation, which will serve as validation in future phases.

Clean Orchard Apple Datasets

The same protocol and tools were used as in the previous campaign, described in D3.1 (Figure 2.1, Figure 2.3). The only difference is that no ground truth data was collected, as only negative images from different angle views were needed to use in this model.

Table 2.1 Clean Orchards Dataset Summary

High-Resolution RGB datasets	Localisation	Resolution
Dataset 1	Zottegem (Belgium)	8192x 5460
Dataset 2	Zottegem (Belgium)	8192x 5460

Orange Dataset

In Spain, two data acquisition campaigns were conducted on Valencia late orange orchards over 5 plots. A pre-harvest campaign in March was performed when the orchards were ready to be harvested. This campaign focused on detecting total yield (number of healthy oranges), damaged oranges on the trees as well as oranges on the ground. The post-harvest campaign aimed at identifying the fallen oranges on the ground and uncollected, remaining oranges on the trees. Aerial acquisitions were performed with a DJI M350 UAV and included high-resolution RGB images (Sony ILX-R1) and LiDAR data (DJI L2), both at nadir and 50° angles. All flights were conducted at 12 meters flight altitude to get optimal resolution (GSD). Ground truth measurements were collected by ESPIGOL.

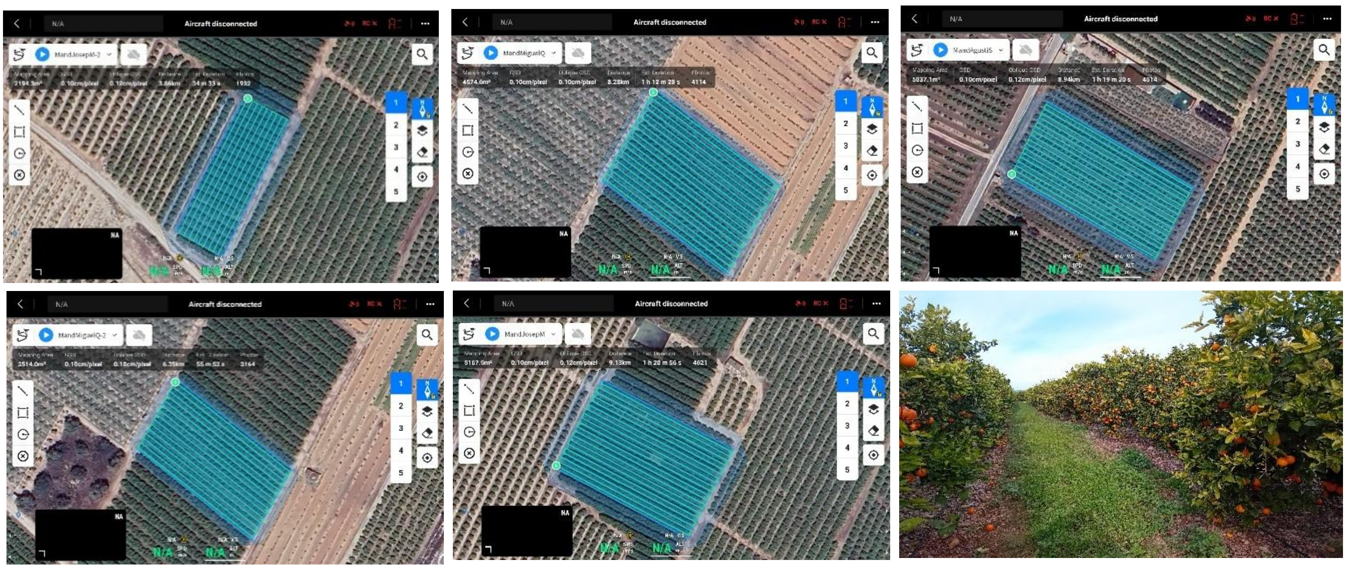

Figure 2.1 UAV mission plans and field view for orange orchard.

Funded by the European Union. Views and opinions expressed are however those of the author(s) only and do not necessarily reflect those of the European Union or the European Research Executive Agency (REA). Neither the European Union nor the granting authority can be held responsible for them.

Figure 2.2 M350 RTK drone in orange orchards: Sony RGB camera (Left) and LiDAR sensor (Right).

Figure 2.3. Preharvest campaign: Example orchard images: left, nadir view; right, oblique view at 50°.

Table 2.2 Overview of orchard plots, areas, and tree sampled counts

Plot	Area(ha)	Sampled Trees	Longitude	Latitude
Plot 1	0.5	24	40.54302	0.41426
Plot 2	0.25	10	40.54172	0.414121
Plot 3	0.5	38	40.53652	0.42574
Plot 4	0.5	24	40.54630	,0.40953
Plot 5	0.25	10	40.54565	0.40903

Figure 2.4. Postharvest campaign: Example orchard images: left, nadir view; right, oblique view at 50°.

Funded by the European Union. Views and opinions expressed are however those of the author(s) only and do not necessarily reflect those of the European Union or the European Research Executive Agency (REA). Neither the European Union nor the granting authority can be held responsible for them.

2.2.2 Brief overview of processing

The apple dataset has been fully annotated and processed using the processing pipeline detailed in D3.1, section 2.2.4 ("Data preparation"). Before annotation, relevant subregions were extracted from the full-resolution UAV images. These subregions were selected to include canopy areas likely to contain visible or damaged fruits, reducing unnecessary annotation work while keeping the high image detail needed for fruit detection. Python scripts were used to crop the selected regions and store their coordinates, allowing each crop to be linked back to the original UAV image. The orange dataset will follow the same processing logic. The orange dataset will follow the same established pipeline.

2.2.3 Method development activities

The method-development workflow follows the strategy described in D3.1. Detection models are developed and tested to identify good, damaged, and fallen fruits. Hence, both YOLO-based and RCNN-based approaches have been implemented and are currently being improved through fine-tuning, hyperparameter optimization, and additional data augmentation strategies (Hu et al., 2023). Also, datasets acquired from different viewing angles are compared to evaluate their effect on fruit visibility and detection accuracy. The next step is to combine multi-angle information and upscale the approach from image-level detection toward orchard-level food loss estimation.

2.3 First Results

2.3.1 Oblique view vs Nadir view (Apple orchards)

The annotations of the apple data (data collect before harvest) over all the sites clearly demonstrate the advantages of oblique (50°) views over nadir (90°) views in terms of both the number of apples that can be seen and in terms of the visibility (quality) with which the apple can be seen. As shown in Figure 2.5, the mean number of annotated apples per image is substantially higher in oblique views (278.5 ± 199.2) compared to nadir views (122.0 ± 66.9). A statistical t-test confirms that this difference is highly significant ($t = 7.41$, $p = 2.6 \times 10^{-11}$), demonstrating that oblique views consistently provide more visible apples than nadir views.

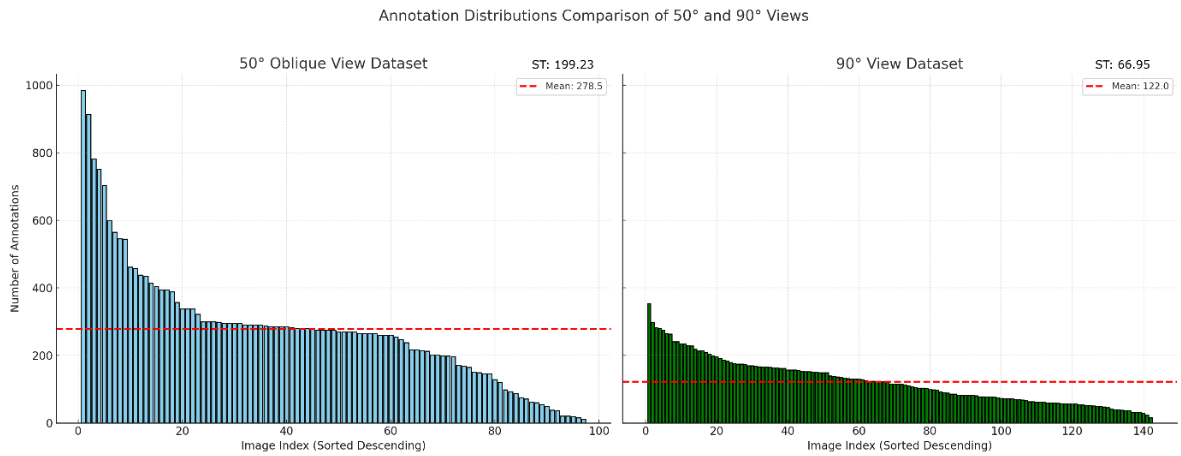

Figure 2.5 Annotation distributions comparison of 50° and 90° viewing angles. This table contains all annotations of all sites of apple (pre-harvest).

Funded by the European Union. Views and opinions expressed are however those of the author(s) only and do not necessarily reflect those of the European Union or the European Research Executive Agency (REA). Neither the European Union nor the granting authority can be held responsible for them.

As mentioned in the previous deliverable, a visibility attribute was used in the annotation operation. Hence a visibility class was assigned to each apple: Class A : good visibility (>50% of the apple can be seen); Class B : medium visibility (between 20 and 50% of the apple can be seen); Class C: Poor visibility (less than 20%).

Figure 2.6 Apple visibility classes, ranging from clearly visible (Class A) to partially visible (Class B) and poorly visible (Class C)

Further analysis based on the visibility attribute (by apple class (good, damaged, and fallen) demonstrates that the oblique view allows greater visibility of apples than the nadir view.

As presented in Figure 2.7, oblique view 50°(right) have a higher proportion of apples with good visibility (Class A), while nadir views contain more partially or poorly visible apples (<20%) (Figure 2.7, left). For example, in oblique views, 17.2% of good apples and 21.8% of fallen apples are highly visible, compared to only 11.0% and 16.9% in nadir views, respectively.

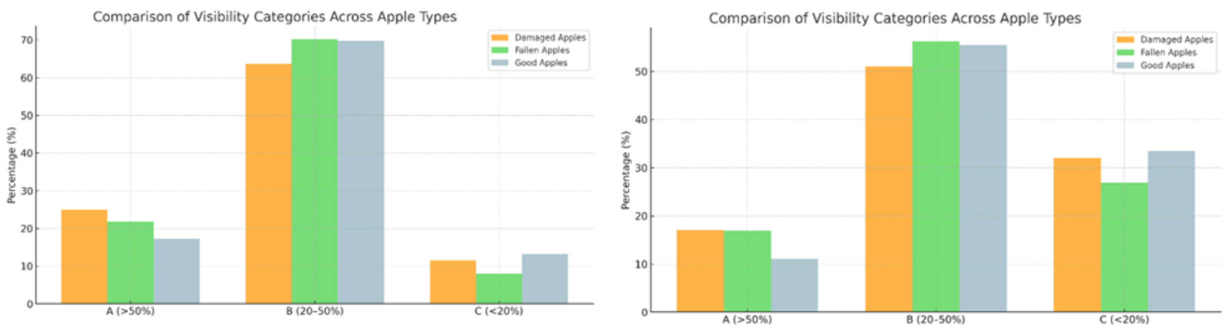

Figure 2.7. Apple visibility in the nadir view (left) and the 50° oblique view (right).

These results highlight that using the 50° oblique view reduces occlusion effects and improves the overall completeness of apple annotations, which is essential for accurate food loss estimation and future detection model development.

2.3.2 Detection Model Performance

The goal is to develop a model that is able to detect all kind of apples, thus being capable of making the difference between good apples, damaged apples hanging in the trees and the apples fallen in the ground.

All models were trained on data from four orchards and evaluated on a separate orchard dataset, demonstrating the generalization performance of the models and highlighting areas for further improvement. The models used YOLOv11 (Wang et al. 2024) and the experiments were performed on the three classes: good apples, fallen apples, and damaged apples using initially Nadir view.

Funded by the European Union. Views and opinions expressed are however those of the author(s) only and do not necessarily reflect those of the European Union or the European Research Executive Agency (REA). Neither the European Union nor the granting authority can be held responsible for them.

Table 2.3 illustrates that for good and fallen apples, the results are promising with the highest recall of 0.74 and a precision of 0.72. However, the class of damaged represent the challenging class, where both precision and recall are low. These results in general suggest that YOLOv11 works reliably for good and fallen apples, while further improvement is needed regarding the detection of damaged apples, possibly by including more training data or selective model refinement and exploring other detection models such as Faster RCNN (Kang & Chen, 2020). These values should be interpreted in light of the t of the imaging and experimental settings (image resolution, occlusion level, acquisition geometry, and class balance). Given the typical challenges of UAV orchard imagery, such as occlusions, background clutter, and illumination variability, the precision and recall values in this range are a promising outcome. Moreover, the scores were achieved on a completely independent orchard dataset that was not included during training, which supports the robustness of the approach and its ability to generalize beyond a single site

Table 2.3. Apple Detection: Test performance per class of Precision and Recall for the YOLOv11 on pre-harvest data.

Class	Precision	Recall
Good apple	0.71	0.65
Fallen apple	0.72	0.74
Damaged apple	0.51	0.52

The multi-class confusion matrix (Figure 2.8) shows good performance on good and fallen apples but confusion with background, mainly because apple colour can be visually similar to surrounding leaves and branches, and because shadows and occlusion reduce apples visibility. Damaged apples remain the most difficult class, with frequent confusion with good apples and background. Overall, the model performs well on good and fallen apples and can be improved by reducing the False positives, through the inclusion of more diverse negative samples during training. False negatives will be further minimized by refining the model and improving its ability to capture challenging cases.

Building on this progress, the model will be continuously improved, including the oblique views to improve the results of the detection and ensure optimal quantification of the loss. Moreover, the best model to oranges using transfer learning will be adapted, so that the approach can be extended to a wider range of fruits and vegetables while requiring only a relatively small amount of additional labelled data.

Funded by the European Union. Views and opinions expressed are however those of the author(s) only and do not necessarily reflect those of the European Union or the European Research Executive Agency (REA). Neither the European Union nor the granting authority can be held responsible for them.

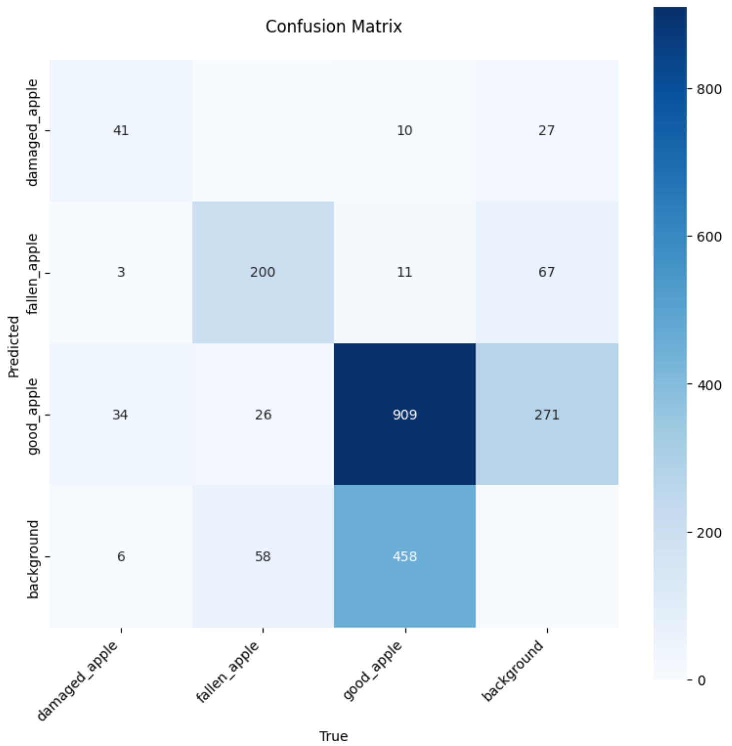

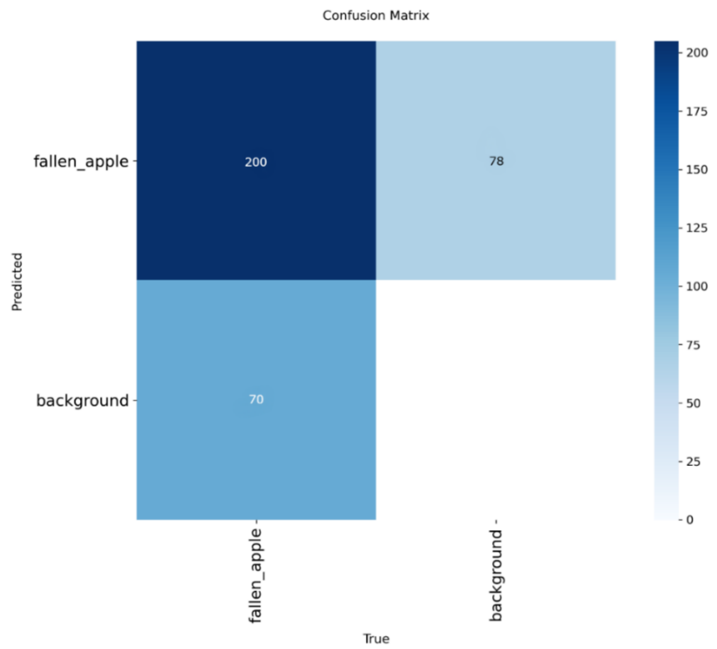

Figure 2.8. Multi-class confusion matrix for the Apple pre-harvest datasets using Nadir imagery (top). Confusion matrix on independent test-set (Fallen apples) (bottom).

Funded by the European Union. Views and opinions expressed are however those of the author(s) only and do not necessarily reflect those of the European Union or the European Research Executive Agency (REA). Neither the European Union nor the granting authority can be held responsible for them.

2.4 Discussion

2.4.1 Results vs original goal

The first results provide a strong and necessary foundation for developing a food loss estimation approach. Having a model that can accurately detect good, damaged, and fallen apples is essential to obtain reliable food loss estimates.

These outcomes show that we are on track with the original goal of creating robust detection tools to support precise quantification of losses in orchards.

2.4.2 Key successes and bottlenecks

The main successes so far include the complete annotation and processing of the apple datasets, as well as the development of object detection models using different approaches (YOLO, Faster RCNN, and Mask RCNN). In addition, two data acquisition campaigns were successfully conducted on oranges in Spain, which will support the generalization of the models to other fruits. First results have been obtained, but further improvements are needed through iterative fine-tuning, advanced hyperparameter optimization, and additional data enhancements.

Despite these successes, some bottlenecks remain. Model optimization, particularly for RCNN-based approaches, is challenging and requires extensive fine-tuning. Handling occlusion and ensuring generalization across different orchards and varying conditions still need further work.

Additionally, processing high-resolution images is computationally demanding and requires significant resources. Finally, preparing large, high-quality annotated datasets is time-consuming and labour-intensive which affects the model development.

Finally, the number of damaged fruits in the dataset is very low (less than 5%), making the detection of damaged fruits particularly challenging.

2.4.3 Further steps and planning

In the next phase, we will continue improving our detection models through fine-tuning, parameter optimization, and data enhancement. A key focus will be on combining images captured from different viewing angles to overcome occlusion and improve detection accuracy. For oranges, the next steps are to process and annotate the collected datasets using the same pipeline developed for apples. This will support model adaptation and validation across different fruit types. Ground truth measurements which are essential for accurate food loss estimation will also be incorporated, working closely with ESPIGOL.

Furthermore, we aim to evolve from detection in individual images to reliable counting at the canopy level by integrating multi-angle data. We will develop a correction method to account for occluded (invisible) fruits, explore model generalization for broader scalability, and define a robust sampling strategy to ensure representative and efficient data collection. Finally, a sampling protocol will be established to define the optimal sampling strategy.

Funded by the European Union. Views and opinions expressed are however those of the author(s) only and do not necessarily reflect those of the European Union or the European Research Executive Agency (REA). Neither the European Union nor the granting authority can be held responsible for them.

2.4.4 Policy recommendations

The initial results suggest that UAV-based high-resolution imagery and deep learning could support more objective fruit loss assessment in orchards. To ensure reliable and comparable results, policy frameworks should support the creation of common protocols for image acquisition, annotation, ground truth collection, and validation. For operational use, the training data collection should be further expanded to include different cultivars, but also larger range in acquisition time, illumination, and differences in orchard structure and farmer practices, to improve the reliability and robustness.

Funded by the European Union. Views and opinions expressed are however those of the author(s) only and do not necessarily reflect those of the European Union or the European Research Executive Agency (REA). Neither the European Union nor the granting authority can be held responsible for them.

3. Repeated multispectral and satellite data for production loss assessment in potato, maize, corn, faba bean and sunflower (Uni-VPM and UGent, T3.2 & T3.3)

3.1 Overview

The goal of this task is to evaluate the impact of various agronomic management practices on food loss at the primary production stages in herbaceous crops, using durum wheat, faba bean, maize and sunflowers as target crops. To achieve this, multispectral data collected regularly throughout the growing season from either UAVs (T3.2) or satellite (T3.3) data are used as input, and combined with radiative transfer models and crop growth models to estimate production (yield) and production losses (See Fig. 3.3 for the interpretation of production losses in this particular task). To calibrate and verify the models, field experiments were carried out.

These were carried out in Belgium (UGent) on potato, and in Italy (UniVPM) on winter wheat, maize, faba bean and sunflower rotation. The experimental set-up was different, but the measurements on the plants and the remote sensing data were completely aligned. Results are presented here from both cases.

Timeline (M01–M42):

- M01–M12: Experimental set-up and initial data collection
- M13–M24: Continued experiments, data processing and methods establishment.
- M25–M42: Experiments and data processing + development of radiative transfer and crop growth modelling

3.2 Materials & Methods

3.2.1 Collected Data (season 2024-2025)

As in the previous years (See D3.1), field experiments were set up by UniVPM (Italy) and by UGent (Belgium) and were followed up. Of the collected data, two types are relevant within this WP, in particular UAV remote sensing data (multitemporal multispectral and thermal imagery) and soil and plant measurements for reference. We here will focus particularly on the remote sensing data.

In Italy, the data collection campaign described in D3.1 is continued at the experimental farm “Pasquale Rosati” of the Polytechnic University of Marche (43°32’39.8” N, 13°21’39.5” E), located in Agugliano, Ancona province, Italy. The open-field trial, established in April 2023, comprises two experimental sites: (i) a plot trial area, consisting of three adjacent and homogeneous fields (120 × 30 m each), and (ii) a calibration field area, made up of four fields of 1 ha each. The data collection for the 2024–2025 growing season has been completed for all three management practices tested in the plot trials—business as usual (BAU), enhanced conventional (ECV), and zero-stress (ZST)—and for BAU also in the calibration fields.

Funded by the European Union. Views and opinions expressed are however those of the author(s) only and do not necessarily reflect those of the European Union or the European Research Executive Agency (REA). Neither the European Union nor the granting authority can be held responsible for them.

In Belgium, a field trial on potato was conducted at the experimental farm of Ghent University in Bottelare (50°57'48.6" N 3°45'39.4" E). The field trial is a three-factor experiment, with Variety, Biostimulant application and Fertilization as factors. It was repeated in 2023, 2024 and 2025.

More details about experimental trials, protocol and previous data campaigns are available in D3.1.

In-field measurements

The same basic ground measurement protocol was applied at both experimental sites for field data campaign. Surveys were conducted at critical phenological stages for each crop. At both sites, crop LAI was measured with a ceptometer (AccuPAR LP-80, Decagon Devices, Inc., Pullman, WA, USA), taking three measurements per plot randomly distributed avoiding borders. Leaf chlorophyll content was measured with a SPAD-502 meter (Konica Minolta, Belgium) on three (wheat trial) and ten (potato trial) fully sunlit, randomly selected leaves per plot avoiding borders. Both the LAI and SPAD readings were conducted on the same date as the UAV flight. Phenology was also recorded along the measurements.

Additional measurements performed in Italy included plant height, leaf gas exchange (transpiration, stomatal conductance, leaf temperature and net photosynthesis) (Figure 3.1). Crop yields are available for wheat, faba bean, sunflower and maize. In addition, for wheat also data on yield components (protein content, 100 grains weight, harvest index) are available, while analyses are still ongoing for maize and sunflower. For potato, yield and yield components were also measured

Figure 3.1 Top: wheat and maize plots in the plot trial; Bottom: measurements of leaf chlorophyll content and leaf gas exchange on sunflower in the plot trial.

Remote sensing

In Italy, during the 2024-25 growing season, both the plot trial and calibration field areas were monitored by remote sensing with a DJI Matrice 350 RTK drone equipped with multispectral sensors (MicaSense Altum, MAIA S2, WV2). Downwelling Light Sensors ensured radiometric accuracy, and flights were scheduled concurrently with ground-based

Funded by the European Union. Views and opinions expressed are however those of the author(s) only and do not necessarily reflect those of the European Union or the European Research Executive Agency (REA). Neither the European Union nor the granting authority can be held responsible for them.

surveys to capture critical phenological stages. Eight flights (14/03, 08/04, 06/05, 28/05, 11/06, 25/06, 10/07, 23/07/2025) were processed in Agisoft Metashape to generate orthomosaics and calculate vegetation indices (Figure 3.2).

At the Belgian experimental site, UAV hyperspectral flights were conducted using the DJI Matrice 600 drone equipped with a SPECIM AFX10 camera (SPECIM, Spectral Imaging Ltd., Oulu, Finland) on a Gremsy T7 gimbal (Gremsy, Ho Chi Minh City, Vietnam) in 2024 and 2025; here, we report on 4 flights in each season.

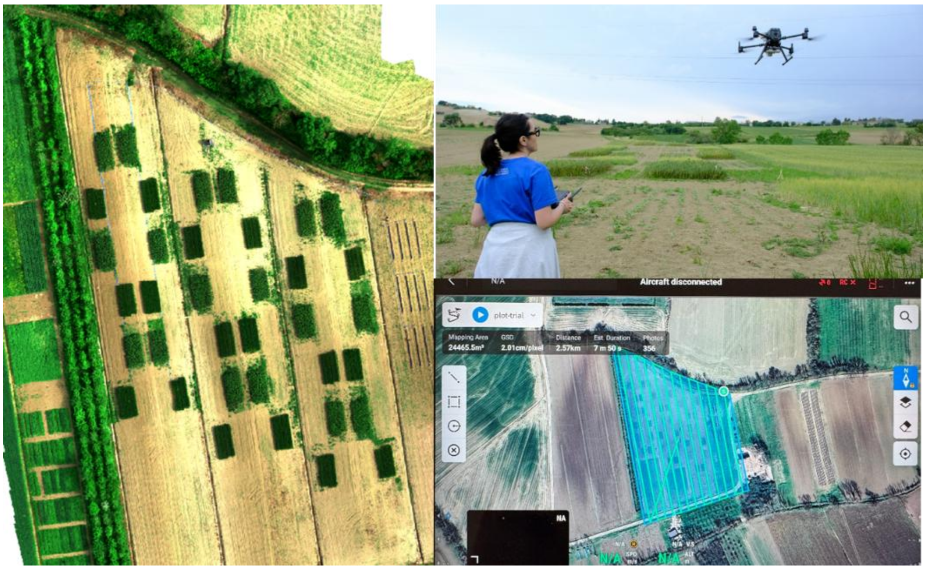

Figure 3.2 Orthomosaic of the trial plots, details of the flight using the DJI Matrice 350 RTK drone, and the flight plan over the plots trial.

<u>Modelling approach</u>

The principle behind the modelling approach is shown in Figure 3.3. Yield can best be estimated using a crop growth model. Such a model uses calibrated crop characteristics, soil type, weather and crop management data to estimate productivity (yield). It estimates plant size (plant height, plant leaf area, chlorophyll content) during the course of the growing season, and based on this calculates the productivity. However, these models do not take actual abiotic and biotic stressors into account. As such, the yield they produce can be understood as a maximally attainable yield in the given conditions.

In this project, we use remote sensing data to regularly recalibrate the crop growth model. This way, the model is adjusted to the actual plant size. The predicted yield can be considered as the actual attained yield. The difference of the attainable and the attained yield, is the production loss.

However, remote sensing multispectral data cannot serve as direct inputs of these crop growth models. A second type of model is needed to translate the spectra and vegetation indices from the remote sensing to the plant size, used to recalibrate the crop growth model. This second type of model is a radiative transfer model. Radiative transfer models are models that predict reflectance and vegetation indices of a plant canopy with known properties (e.g., plant height, plant leaf area, chlorophyll). Through an inversion of this model using a look-up-table (LUT), the leaf area index and chlorophyll content can be derived from the remote sensing data.

Funded by the European Union. Views and opinions expressed are however those of the author(s) only and do not necessarily reflect those of the European Union or the European Research Executive Agency (REA). Neither the European Union nor the granting authority can be held responsible for them.

In this Deliverable report, the focus will be on the radiative transfer model.

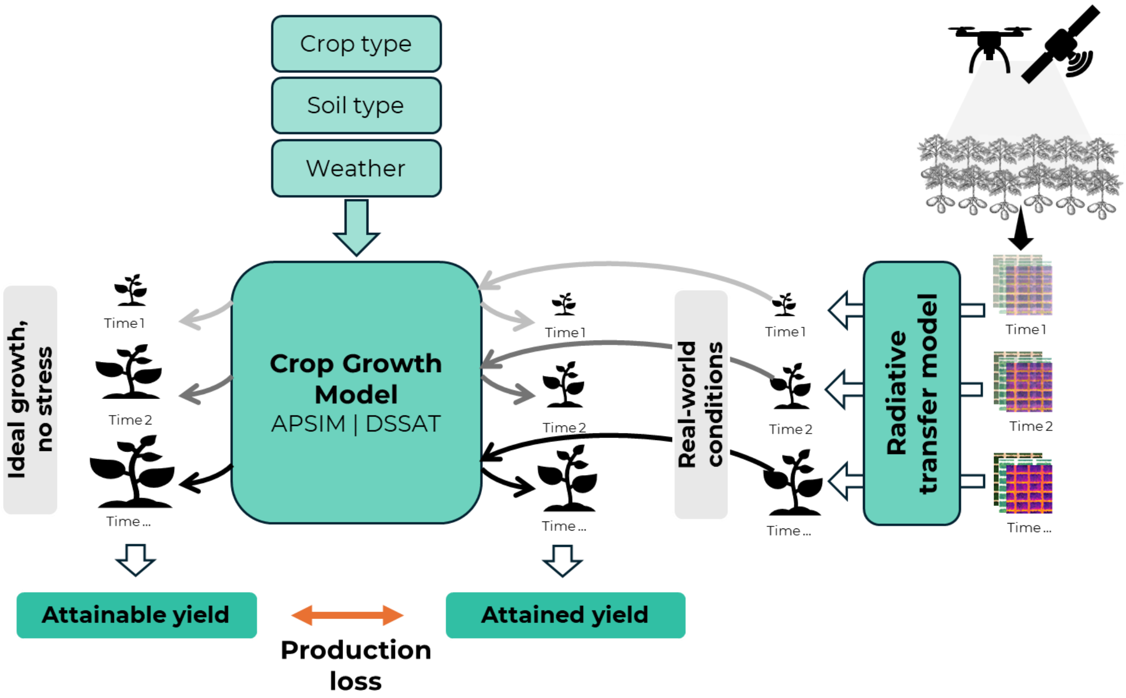

Figure 3.3 Schematic representation of the modelling approach, coupling a radiative transfer model and a crop growth model to attain production loss.

Radiative transfer model

The SCOPE model is an integrated radiative transfer and energy balance framework designed to simulate the spectral signature of vegetated surfaces across the visible, near-infrared, short-wave infrared, and thermal spectral ranges (400–2500 nm), with adjustable spectral resolution (van der Tol et al., 2009). In this study, the retrieval was carried out by inverting forward RTMo of SCOPE using a LUT approach. SCOPE 2.0 was used and executed in MATLAB R2024b.

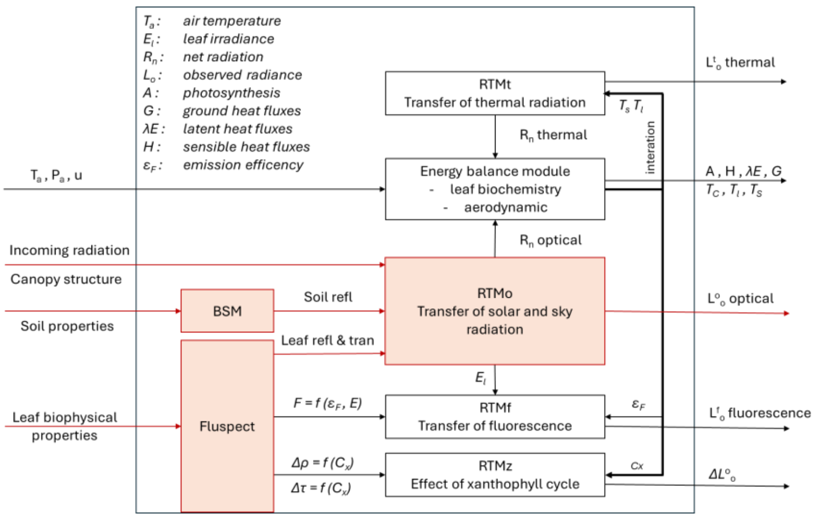

Figure 3.4 Conceptual scheme of the SCOPE model (from Yang et al. 2020) and the corresponding table of acronyms. The modules, inputs, and outputs used in this study are highlighted with a red frame.

Funded by the European Union. Views and opinions expressed are however those of the author(s) only and do not necessarily reflect those of the European Union or the European Research Executive Agency (REA). Neither the European Union nor the granting authority can be held responsible for them.

To generate the LUTs, the SCOPE model was run in forward mode to simulate reflectance for an appropriate set of parameter combinations (see Figure 3.4). The LUTs consist of approximately 100,000 parameter combinations, chosen as a good compromise between computational resource requirements and the accuracy of leaf parameter estimation (Weiss et al. 2000; Duan et al. 2014). The same LUTs were used for LAI and Cab estimation for both crops. The 100,000 parameter combinations were generated by systematically varying selected parameters within specified ranges and fixed steps, while other parameters were held constant.

The ranges of the parameters (Table 3.1) for wheat and potato were selected based on prior field information to constrain the range and force the results toward the mean of measured values (Celesti et al. 2018; Zhu et al. 2019), as well as on literature findings. LUTs were generated for each day of field and UAV flights campaign due to different solar zenith angles.

Table 3.1. Ranges of the input parameters for the SCOPE model for the generation of the LUTs

Parameter	Name and source	Unit	Range for wheat	Range for potato
Variable	Leaf Chlorophyll Content (Cab)[1]	μg/cm²	25–65	10–50
	Equivalent water thickness (Cw)[2]	cm	0.001–0.035	
	Dry matter content (Cm)[3]	g/cm²	0.001–0.0085	0.003–0.011
	Leaf structure parameters (N)[4]		0.5–3	1–2
	Leaf Area Index (LAI)[1]	m²/m²	0.3–7	0.5–5.5
Constant	Equivalent water thickness (Cw)[5]	cm		0.02
	Leaf Inclination Distribution Function (LIDF)[6]		Based on phenological stage	
	Solar Zenith Angle (SZA)	Degree	Based on UAV's flight schedule	

[1] Field data campaign; [2]Longmire et al. 2022; [3]Longmire et al. 2022; Li et al. 2023; [4]Duan et al. 2014; Longmire et al. 2022; [5]Prikaziuk et al. (2022); [6] Planophile, Erectophile, Plagiophile, Extremophile, Spherical, Uniform

After converting the LUT spectral profiles into simulated reflectance matching the specific cameras, the solution to the inverse problem was derived at the polygon level, with each polygon representing an experimental plot, by sorting the LUT entries for each polygon according to a cost function.

3.3 Results

3.3.1 Potato (Belgium)

The radiative transport model based on the hyperspectral data was able to reproduce LAI in potato reliably, both in terms of the seasonality and the absolute values. This is illustrated in Figure 3.5 for the two different nitrogen treatments. For 2025, similar results were obtained. For the chlorophyll content (Cab), slightly poorer results were obtained (Figure 3.6), which can be related to the fact that the reference measurements for Cab were indirect measurements through SPAD measurements. Overall, there is still a clear linear relationship between both datasets, and the temporal dynamics are also very similar.

Funded by the European Union. Views and opinions expressed are however those of the author(s) only and do not necessarily reflect those of the European Union or the European Research Executive Agency (REA). Neither the European Union nor the granting authority can be held responsible for them.

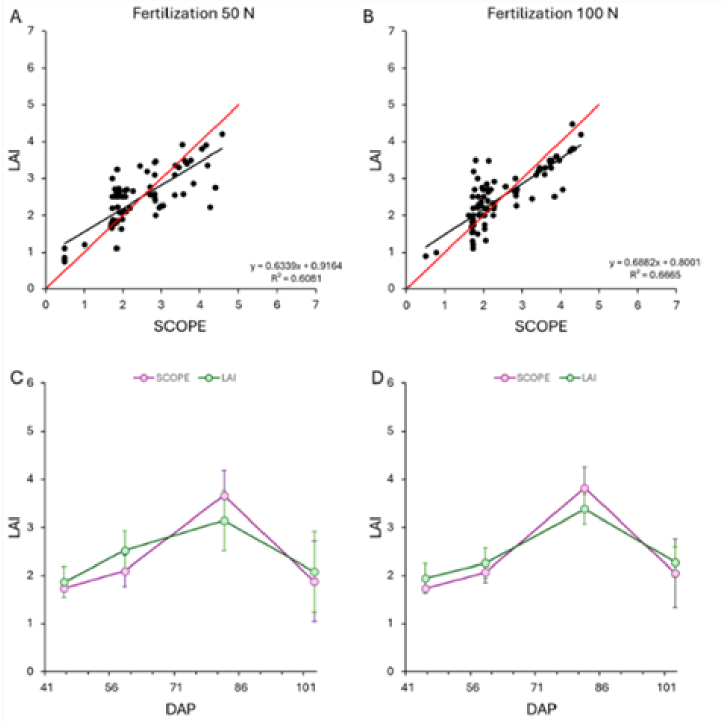

Figure 3.5 ***A,B*** *Scatterplot between the measured leaf area index (LAI) and the modelled content using SCOPE for potato in the 2024 field experiment, for the two N treatments (50 N = 50% nitrogen fertilization; 100 N = 100% nitrogen fertilization). The red line is one-to-one line, and black line is the linear regression line.* ***C,D*** *Time series of the observed and simulated LAI for both treatments (x-axis days after planting (DAP), y-axis values of Cab). Bars represent standard deviation of the means.*

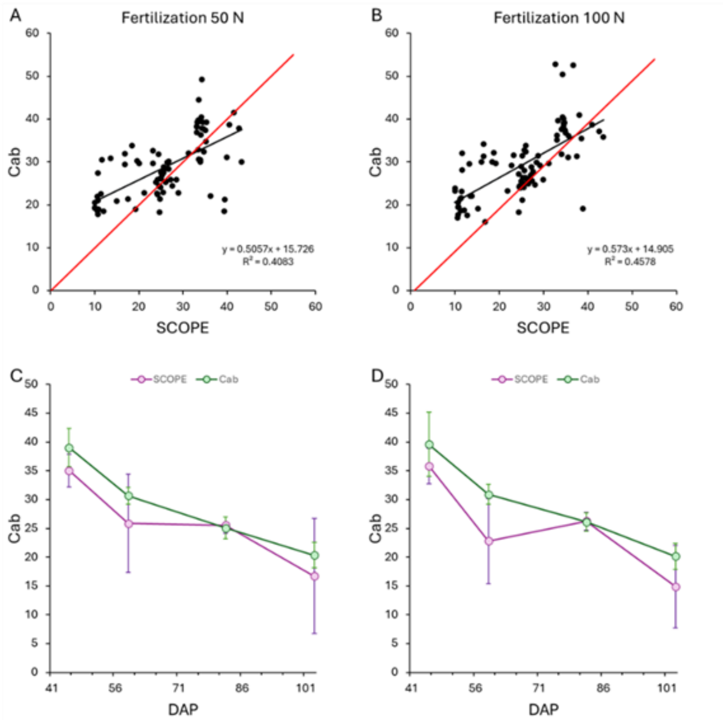

Figure 3.6 ***A,B*** *Scatterplot between the measured chlorophyll content (Cab), derived from SPAD values, and the modelled content using SCOPE for potato in the 2024 field experiment, for the two N treatments (50 N = 50% nitrogen fertilization; 100 N = 100% nitrogen fertilization). The red line is one-to-one line, and black line is the linear regression line.* ***C,D*** *Time series of the observed and simulated Cab for both treatments (x-axis days after planting (DAP), y-axis values of Cab). Bars represent standard deviation of the means.*

Funded by the European Union. Views and opinions expressed are however those of the author(s) only and do not necessarily reflect those of the European Union or the European Research Executive Agency (REA). Neither the European Union nor the granting authority can be held responsible for them.

3.3.2 Winter wheat (Italy)

The estimate of leaf area with the multispectral overall resulted in good estimates, with R^2-values between measured and simulated LAI varying between 0.50 and 0.66 for the two different growth years and treatments. This is illustrated in Figure 3.7 for the business-as-usual treatment; trends for the Zero Stress treatment were similar. Notice also that the dynamics are also very similar, with the exception of the last measurement in 2025.

As for potato, results were slightly worse for Cab estimates (Figure 3.8). In both years, Cab was overestimated with SCOPE, although dynamics were still accurately represented. Again, this can also partially be attributed to the indirect nature of the Cab measurements using SPAD data. In addition, Cab values were relatively high and constant throughout. Nevertheless, the very steep slope between SCOPE simulations and actual SPAD levels indicates that the distribution in SCOPE is even more limited than actually measured. This was also the case for the Zero Stress treatment, but improved markedly in 2025. The total chlorophyll content CCab, calculated from the product of LAI and Cab, is a more important value as input in the crop growth models, and was predicted with better accuracy in both years (R^2 between 0.37 and 0.73).

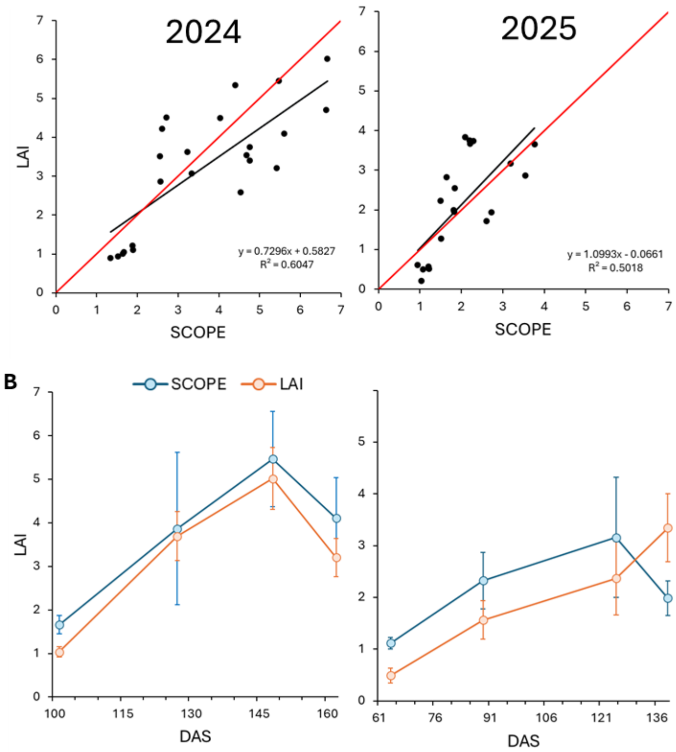

Figure 3.7 Performance of SCOPE to predict LAI in winter wheat for the business-as-usual treatment. ***A*** *Scatterplot between observed and simulated LAI for 2024 and 2025. The red line is one-to-one line, and black line is the linear regression line.* ***B*** *Time series of the observed and simulated LAI for both growing years.*

Funded by the European Union. Views and opinions expressed are however those of the author(s) only and do not necessarily reflect those of the European Union or the European Research Executive Agency (REA). Neither the European Union nor the granting authority can be held responsible for them.

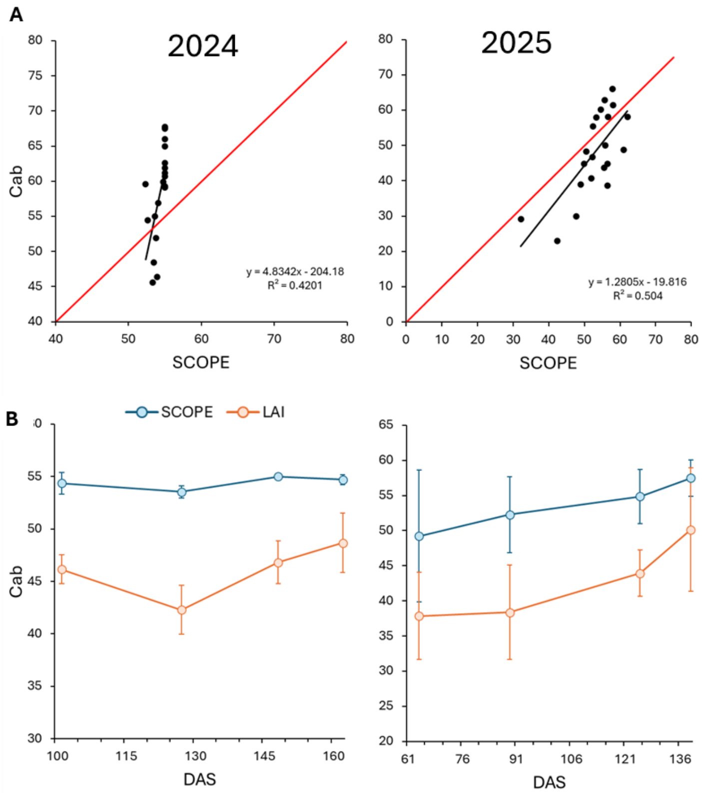

*Figure 3.8 Performance of SCOPE to predict Cab in winter wheat for the business-as-usual treatment. **A** Scatterplot between observed and simulated Cab for 2024 and 2025. The red line is one-to-one line, and black line is the linear regression line. **B** Time series of the observed and simulated Cab for both growing years.*

3.4 Discussion

The study conducted within this Task demonstrates the effectiveness of UAV multispectral and hyperspectral imagery for RTM inversion and shows that the SCOPE model can reproduce measured values, track the seasonal dynamics of wheat and potato, and capture field-observed patterns under contrasting agronomic management practices.

The estimation of wheat LAI through SCOPE inversion of multispectral UAV imagery proved promising overall, across both growing seasons. The seasonal dynamics were well captured by the model, which correctly identified the vegetative peak at flowerig. SCOPE slightly overestimated low LAI values (<2 m^2 m^{-2}) and underestimated higher ones (>4 m^2 m^{-2}) in wheat, while inversion of UAV hyperspectral data for potatoes performed well. Nitrogen fertilization affected absolute LAI and Cab, with 100 N treatments yielding higher values, though model accuracy changed little. In 2024, SCOPE accuracy was similar between 50 N and 100 N treatments (R^2 > 0.6; RMSE ≈ 0.4 m^2 m^{-2}).

In 2025, despite severe water stress and stronger nitrogen effects on LAI (3.5 vs. 4.7 m^2 m^{-2}), predictive accuracy remained high (R^2 > 0.4; RMSE ≈ 0.6 m^2 m^{-2}). In fact, during dry seasons, differences among fertilization levels become more pronounced because nitrogen supports the maintenance of green leaf area for a longer period, delaying senescence (Webber et al. 2015; Blanc et al. 2024). The high level of accuracy reflects the strong correlation between field canopy structure and hyperspectral reflectance, with a slight underestimation of LAI during emergence and senescence stages and a modest

Funded by the European Union. Views and opinions expressed are however those of the author(s) only and do not necessarily reflect those of the European Union or the European Research Executive Agency (REA). Neither the European Union nor the granting authority can be held responsible for them.

overestimation at intermediate values. The tendency to underestimate high LAI values in both crops can be attributed to reflectance saturation once LAI exceeds ~3 m^2 m^{-2}.

Beyond this threshold, the difference between red and near-infrared reflectance becomes negligible as vegetation density increases. It is well known that both physical and empirical approaches suffer from this limitation, as relationships between inverted LAI and canopy reflectance saturate under high vegetation density.

Additionally, management practices affected inversion accuracy: results were better in BAU than in ZST, with higher R^2 and lower RMSE values. In BAU plots, biotic and abiotic stress led to greater canopy heterogeneity, which enhanced the sensitivity of reflectance to LAI variability (Rivosecchi et al. 2024b).

Conversely, the dense and uniform canopies in ZST plots produced highly similar spectral signatures, intensifying saturation effects and reducing the model's ability to resolve actual differences in LAI. As a result, spectral signatures were highly similar across plots, and spectral saturation limited the model's ability to detect real variations in LAI. In BAU, stress factors (nitrogen deficiencies and mainly water stress, although ultimately both growing seasons were favourable from this perspective) introduced greater heterogeneity in LAI and reflectance, facilitating the identification of differences and improving correlations with measured values.

It should be noted that SPAD provides only an indirect estimate of chlorophyll content, as both the measurement itself and the empirical conversion to Cab are inherently uncertain. In contrast, LAI measurements are more direct and thus more reliably reflect canopy structure. Indeed, leaf chlorophyll content, dynamics were less pronounced, and estimation accuracy was lower in both wheat and potato, although hyperspectral inversion provided comparatively better results. Overall, the model generally underestimated Cab across crops and treatments.

As reported in the literature, LAI estimates proved more accurate than Cab estimates. This higher accuracy is likely because structural variables exert a stronger influence on total canopy reflectance than biochemical variables. Signal propagation from leaf to canopy scale is typically weak, leading to poor estimation of leaf biochemical parameters from canopy-level reflectance.

Furthermore, chlorophyll variation is only captured in the visible region, where reflectance has a very narrow dynamic range due to strong absorption. This increases the likelihood of errors in SCOPE simulations of visible reflectance, and consequently in Cab retrieval.

Previous studies have shown improved robustness and accuracy when biochemical variables are estimated at the canopy level (e.g., canopy chlorophyll, defined as Cab * LAI) rather than at the leaf level supporting that remote sensing provides stronger representativeness at the canopy scale, while its accuracy in resolving leaf-scale biochemical traits remains limited. This suggests that chlorophyll retrieval at the leaf scale is generally less reliable than at the canopy scale.

Consistently, in this study, better results were obtained for canopy chlorophyll content compared to its individual components (i.e., LAI and Cab) across both wheat and potato growing seasons.

Funded by the European Union. Views and opinions expressed are however those of the author(s) only and do not necessarily reflect those of the European Union or the European Research Executive Agency (REA). Neither the European Union nor the granting authority can be held responsible for them.

3.4.1 Results vs original goal

The results of this study are still aligned with the original goal.

3.4.2 Key successes and bottlenecks

In both sites, the field trials as such have delivered relatively good results, in line with project expectations, and the experimental protocol is proving highly effective. Moreover, the successful calibration and validation of the crop model open up promising opportunities for future applications and scenario analyses.

In parallel, the new drone configuration has significantly reduced the time required for data collection, streamlining field operations and improving efficiency. At the same time, in both sites, the project is managing an exceptionally large volume of data from both ground measurements and remote sensing, covering four different crops and numerous surveys. For the modelling component in particular, calibration and validation demand a very high number of parameters, making the process time-consuming and resource-intensive.

3.4.3 Further steps and planning

What has been presented here are the results of the radiative transfer model inversion, deriving best fits for the most important crop characteristics. Next, these data are used to recalibrate the crop growth model. From this final integration, yield and production losses can be predicted. In the next months, the crop growth model will be integrated with the radiative transfer models to retrieve yield data. A full calibration of winter wheat with the crop growth model DSSAT has been performed for winter wheat.

The next challenge is to repeat the radiative transfer model with satellite data. This will be done by project partner UNIVPM for the winter wheat case. In the next phase of the project, remote sensing data will be leveraged to scale up field observations to a wider level, effectively linking drone-based and satellite-based approaches. This effort will be enhanced by incorporating additional satellite imagery over the calibration field area and by introducing a temporal dimension to represent the data as time series. Greater focus will be placed on spatial assimilation techniques and ensemble strategies to improve the accuracy of crop yield estimates derived from remote sensing. Subsequent steps will involve integrating remote and proximal sensing data with crop growth models (i.e., DSSAT) to assess potential yields under various management and climatic scenarios.

The original goal was always to estimate production losses, but in the course of the project, the new developed definition of food losses actually do not include production losses. In Belgium (partner UGENT), we are studying whether satellite data of potato field losses can be more directly related to losses. In wet years, wet clayey fields can sometimes not be harvested. This was for instance the case in 2023 in areas in Flanders. This results in very high regional losses. UGENT will evaluate whether soil moisture levels, derived from high resolution Sentinel-1 data, in combination with soil texture data, can be used to predict whether fields can be harvested in wet conditions or not.

Funded by the European Union. Views and opinions expressed are however those of the author(s) only and do not necessarily reflect those of the European Union or the European Research Executive Agency (REA). Neither the European Union nor the granting authority can be held responsible for them.

3.4.4 Policy recommendations

The initial results suggest that the integration of multispectral data from UAV and satellite platforms with crop growth and radiative transfer models can provide a robust framework for estimating yield and yield losses for the selected and tested crops. To ensure consistency and scalability, policy frameworks should promote the adoption of standardized protocols for data acquisition, preprocessing, and model calibration across different agro-environmental conditions/management.

In addition, the systematic collection of ground-truth data through coordinated field experiments should be supported to improve model reliability and transferability. Policies should also encourage the integration of these digital tools into advisory systems for farmers, enabling data-driven decision-making aimed at reducing production losses. Finally, investment in open data infrastructures and interoperability standards would facilitate broader adoption and cross-regional comparability of results.

An aspect to consider is also the data governance, including clear rules for data ownership, access rights, sharing mechanisms, and long-term stewardship of agronomic and remote sensing data. In particular, policies should support the development of interoperable data infrastructures aligned with FAIR principles (Findable, Accessible, Interoperable, Reusable), ensuring that datasets can be effectively reused across regions and applications (e.g., EU AG dataspaces).

Funded by the European Union. Views and opinions expressed are however those of the author(s) only and do not necessarily reflect those of the European Union or the European Research Executive Agency (REA). Neither the European Union nor the granting authority can be held responsible for them.

4. Automated fish egg sorting using multispectral camera technology in trout aquaculture (UNIVPM-T3.4)

4.1 Overview

The objective of this task is to assess and, where possible, minimize production losses during the critical phase of the rainbow trout (*Oncorhynchus mykiss*) production cycle, specifically during early embryonic development (fertilized alive eggs). To achieve this, an automated system equipped with multispectral cameras has been developed and validated to enable the early detection, removal, and counting of dead embryos. The initial phase focused on image acquisition using multispectral cameras and the training of a deep learning model using state of art models improving other existing approaches (Rohani et al., 2019, Cardona et al., 2020). Subsequent phases involved the development of vertical incubator prototypes, which were then tested under real farming conditions.

Timeline (M01–M42):

- M01–M12: Basic set-up:
    - Initial test with multispectral camera system for egg sorting
    - First idea for prototype of egg lifting system
- M13–M24: Preparation of next stage:
    - Build and test of Prototypes 1 & 2
    - Preparation of first egg lifting system in an operational fish farm
- M25–M42:
    - First operational test in fish farm
    - Final egg lifting type
    - Preparation of egg sorting robot arm

4.2 Materials & Methods

4.2.1 Collected Data

<u>Preliminary image acquisition and deep learning model training</u>

In this stage, activities were primarily aimed at consolidating the preliminary data reported in D3.1. Data collection continued with the analysis of 50 batches of rainbow trout embryos, supplied by an Italian producer, using XIMEA multispectral cameras (Figure 4.1). For each batch, both viable (orange) and non-viable (white) embryos were arranged in a single layer, and image acquisition was carried out in the visible (VIS) and near-infrared (NIR) spectra. The same procedure was repeated with the embryo layer covered by water to simulate immersion conditions. A total of three images per batch, both with and without water, were collected. These images were then annotated by domain experts using the Labelbox platform and subsequently employed to train the deep learning model.

Funded by the European Union. Views and opinions expressed are however those of the author(s) only and do not necessarily reflect those of the European Union or the European Research Executive Agency (REA). Neither the European Union nor the granting authority can be held responsible for them.

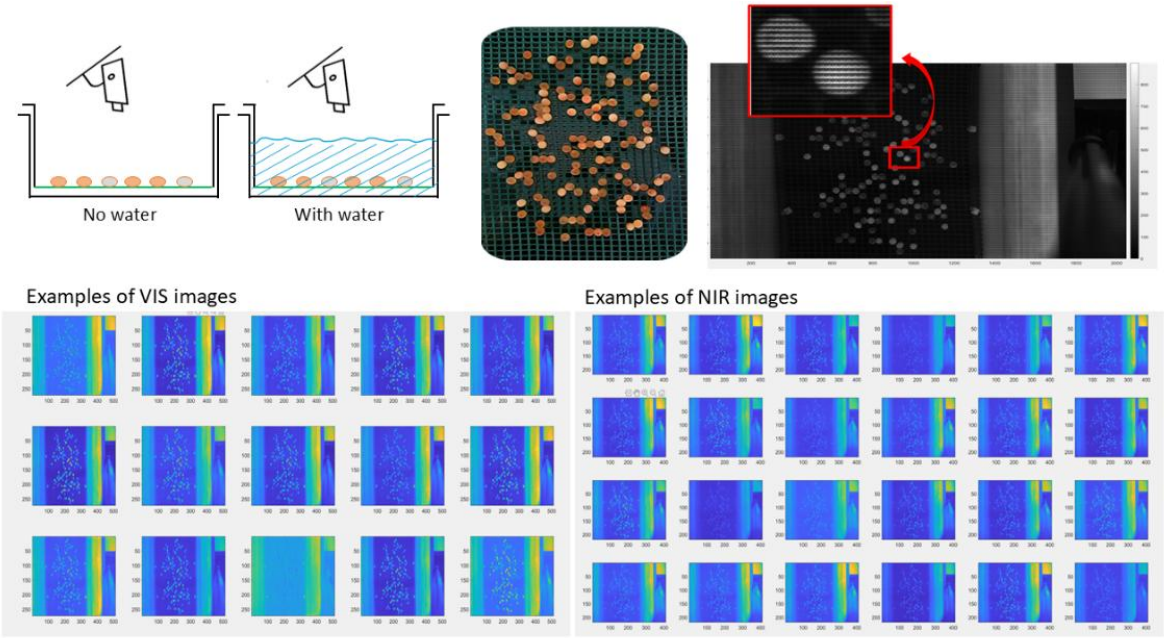

Figure 4.1 Examples of image acquisition set up and VIS and NIR images

Data obtained from the vertical incubator prototype

A vertical incubator prototype integrating computer vision technologies and environmental sensors was developed and tested under commercial farming conditions (Società Agricola Troticoltura F.lli Leonardi, Trento, Italy) over a seven-day period in February 2025.

The prototype (Figure 4.2) featured a vision system based on high-resolution Basler USB 3.0 cameras, capable of capturing both RGB and grayscale images. Image acquisition was managed by a GPU-equipped computer to accelerate the inference time of the deep learning model used for detecting healthy and diseased embryos. Inside the incubator, a motorized screw conveyor set at a 45° angle gently lifted embryos from the base of the system to a sorting area, where multispectral cameras enabled embryo classification.

The prototype also included: (i) a Pacific system (data logger) with probes and sensors for continuous monitoring of water parameters (pH, temperature, dissolved oxygen, and CO_2) to ensure optimal operating conditions; and (ii) a water flow meter to verify correct embryo transport, preventing excessive turbulence or stagnation.

Every day, the embryos underwent one complete passage through the screw conveyor and camera inspection for selection. 10.000 RGB frames related to the testing campaign (Feb'25) have been collected and annotated using the labelbox platform. Only a sub-set of these frames have been manually annotated the generate the dataset that have been used the train a deep learning model.

At the end of the seven-day experimental period, embryos were transferred to conventional vertical hatchery systems for hatching till the hatching moment. A control batch with the same amount of newly fertilized embryos was maintained in traditional hatching systems till hatching, and the hatching ratio was assessed for both batches.

The experiment was run in triplicate and each batch consisted of appproximately 600 embryos each.

Funded by the European Union. Views and opinions expressed are however those of the author(s) only and do not necessarily reflect those of the European Union or the European Research Executive Agency (REA). Neither the European Union nor the granting authority can be held responsible for them.

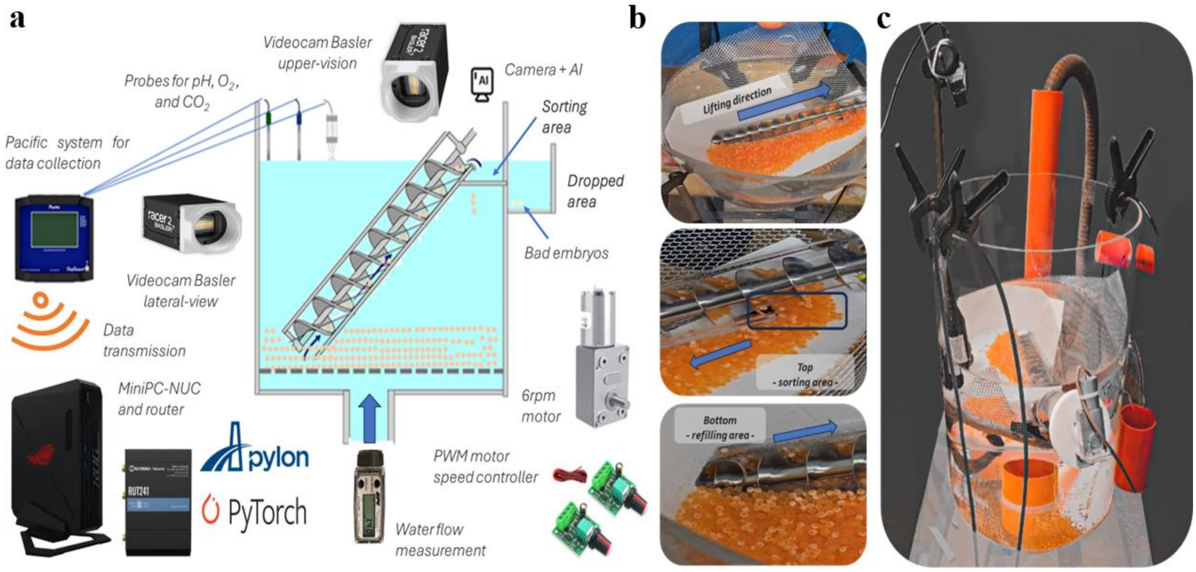

Figure 4.2 (a) Scheme of the prototype; (b) details of the rainbow trout embryos transit in the cochlea, (c) and first prototype assembled in farm conditions.

4.2.2 Brief overview of the data processing

Preliminary image acquisition was carried out to train the deep learning model for egg detection and labelling based on reflectance data. This step was essential to identify the most relevant spectral bands. Data collected during prototype testing under farming conditions were used to: (i) confirm the ability of the cameras to discriminate embryos within the sorting area; (ii) verify that the motorized screw conveyor effectively transported embryos from the bottom of the incubator to the sorting area without compromising their integrity, given their high fragility at this developmental stage; and (iii) compare hatching rates of embryos processed in the prototype system with those of embryos from the same batch reared in conventional hatchery systems.

4.2.3 Method-development activities

A technological prototype of an automated vertical incubator is being developed, equipped with multispectral cameras and dedicated tools designed to gently lift embryos while rapidly identifying and removing non-developing or infected ones.

Following the setup of the imaging acquisition system and the training of the deep learning model, the primary challenge addressed was the gentle lifting of embryos within the incubator to enable their exposure to the cameras positioned in the sorting area at the top of the system. The adopted solution was a screw conveyor (cochlea) tilted at 45°, whose effectiveness was initially validated using plastic beads matching the embryos in size and density (Figure 4.3).

Funded by the European Union. Views and opinions expressed are however those of the author(s) only and do not necessarily reflect those of the European Union or the European Research Executive Agency (REA). Neither the European Union nor the granting authority can be held responsible for them.

Figure 4.3. First test of the cochlea using plastic beads.

The second prototype (Figure 4.4) was subsequently assembled, as detailed in Section: **Data obtained from the vertical incubator prototype**, incorporating the motorized screw conveyor (cochlea), the vision system, and a comprehensive set of environmental sensors for real-time monitoring of water quality and system performance. This version of the prototype was then tested under real farming conditions to evaluate its operational efficiency, embryo handling safety, and overall reliability in a production setting.

The next phase of development will focus on enhancing the system's automation capabilities by integrating a dedicated slide mechanism to accurately direct embryos into the sorting area, as well as a specialized device for the precise removal of non-viable or infected eggs based on data acquired by the multispectral imaging system. These upgrades aim to improve sorting accuracy, reduce manual intervention, and optimize embryo survival rates, ultimately contributing to a more efficient and scalable hatchery management solution.

4.3 First Results

The initial on-farm testing phase was limited to one single trial, because of the hight costs and practical challenges related. However, it demonstrated that the prototype was capable of efficiently lifting and transporting the embryos without causing any visible damage or compromising their integrity, a critical factor given their high fragility at this developmental stage. To have both good and bad embryos, useful to develop a preliminary dataset, the team decided together with the farmer to use medium quality broodstock (variable age, no specific diet for reproduction).

Since the quality of the eggs is a major factor to achieve hatching, heavily influenced by the female parent's health, nutrition, and breeding protocols, this aspect has deeply influenced the final survival rate of hatchlings during our trial. This result was also affected by the selected of the embryo batch which did not undergo the typical initial selection of fertilized and not fertilized eggs. Consequently, during this preliminary trial, a general lower survival rate at hatching was expected.

Funded by the European Union. Views and opinions expressed are however those of the author(s) only and do not necessarily reflect those of the European Union or the European Research Executive Agency (REA). Neither the European Union nor the granting authority can be held responsible for them.

A YOLOv10[1] algorithm was used starting from a pre-trained COCO dataset with a custom training procedure to adapt the model to our specific case. Dataset was manually annotated by experts. Images have been also augmented (rotation, vertical/horizontal flip) to increase the number of samples for each category. The vision system and the first release of the model achieved an overall classification accuracy of 94% circa, successfully distinguishing viable embryos from non-viable or abnormal ones (see Figure 4.4).

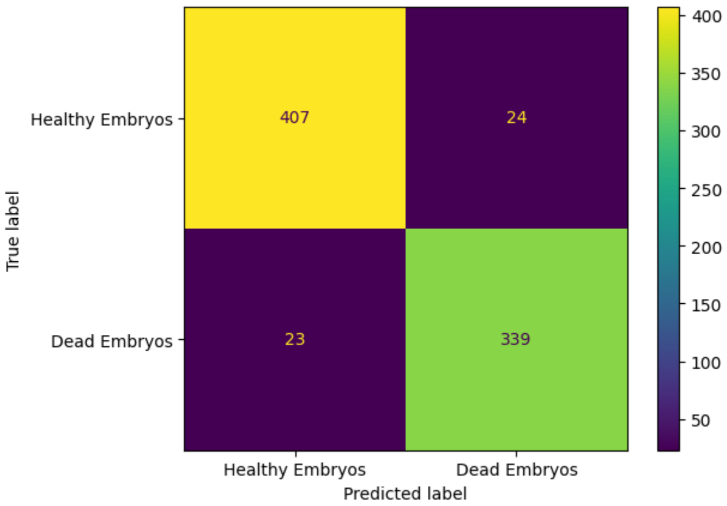

Figure 4.4. Confusion matrix on test-set derived from a 60-20-20 random split on initial dataset (training - validation - test).

At the conclusion of the experimental period, comparative analysis of hatching rates between embryos reared in the prototype incubator and those maintained in standard vertical hatchery systems revealed no statistically significant differences, confirming that the new technology did not negatively affect embryo development or survival. More specifically, the survival rate at hatching of the embryos incubated from the beginning in the conventional hatching system was 46,0 ± 5,0% while those incubated for 7 days in the prototype followed by conventional incubation showed a survival rate of 44,5±6,0%.

Even though survival rates do not look in perfect line with typical values of trout farms, it should be noted that: (i) the lifting system does not affected the final survival rate if compared with standard incubation process (in contrast with the common farm practices that impose no embryo manipulation) ; (ii) the experimental setup was specifically designed to use medium quality egg batches in order to have both good and bad eggs from the beginning of the experiment and test the prototype in sub-optimal conditions (presence of dead embryos from the beginning with possible microbial diffusion). These results validate the potential of the prototype as a safe and effective tool for automated embryo lifting, monitoring and selection in aquaculture operations.

[1] Wang, A., Chen, H., Liu, L., Chen, K., Lin, Z., & Han, J. (2024). Yolov10: Real-time end-to-end object detection. *Advances in Neural Information Processing Systems*, *37*, 107984-108011. https://arxiv.org/abs/2405.14458

Funded by the European Union. Views and opinions expressed are however those of the author(s) only and do not necessarily reflect those of the European Union or the European Research Executive Agency (REA). Neither the European Union nor the granting authority can be held responsible for them.

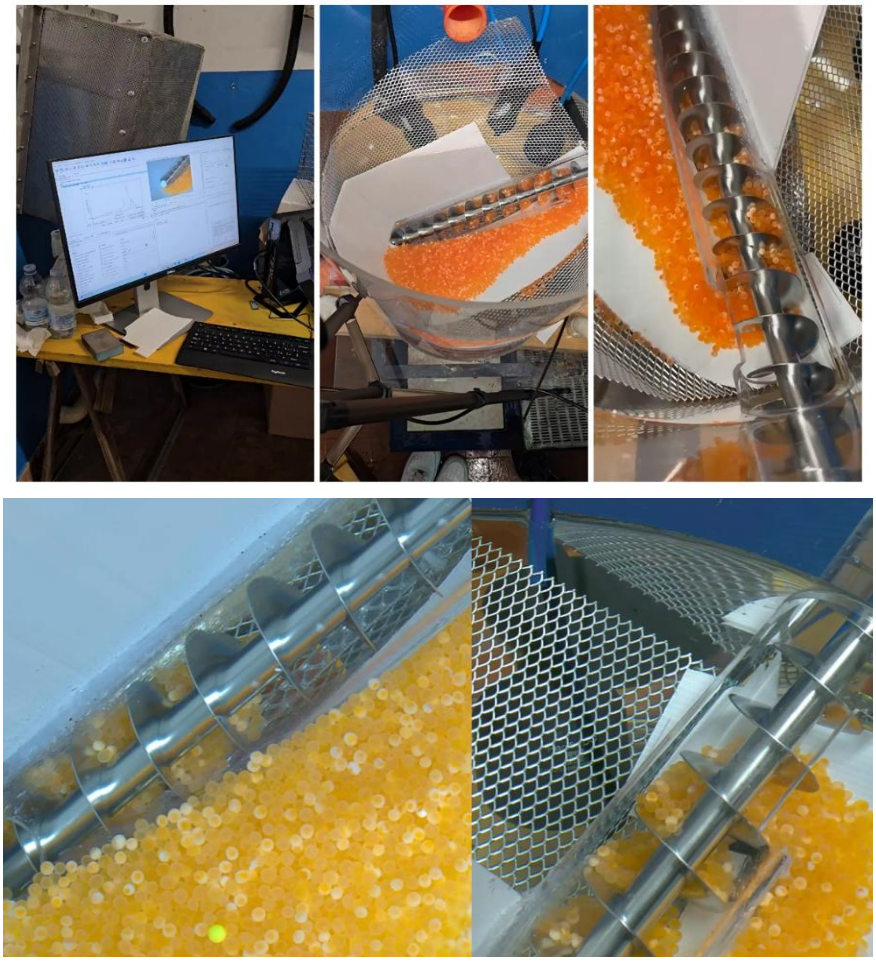

Figure 4.5. Top. Data acquisition during the test of the first prototype in farm conditions. Bottom: example of RGB frame from acquisition system

4.4 Discussion

4.4.1 Results vs original goal

The results obtained from the first round of testing confirm that the prototype is well aligned with the original objective of developing and validating an automated system, based on multispectral imaging, capable of early detection, counting, and removal of dead embryos. The integration of the motorized screw conveyor (cochlea) with the imaging system successfully enabled the gentle handling and full exposure of entire embryo batches to the sorting area, where they were accurately classified.

These findings represent a significant milestone toward the creation of a fully operational prototype capable not only of reliably identifying but also removing non-viable embryos, thereby enabling precise estimation of production loss during this critical stage of the production cycle. Such a system has the potential to minimize embryo losses compared to conventional hatchery practices, contributing to more efficient and sustainable aquaculture management (Lindholm-Lehto & Pylkkö, 2024).

Funded by the European Union. Views and opinions expressed are however those of the author(s) only and do not necessarily reflect those of the European Union or the European Research Executive Agency (REA). Neither the European Union nor the granting authority can be held responsible for them.

4.4.2 Key successes and bottlenecks

The second prototype successfully automated the entire embryo selection process, significantly reducing the need for manual intervention while improving classification accuracy. In addition, continuous monitoring of both embryo development and water quality parameters ensured optimal environmental conditions throughout incubation. The combination of high-resolution imaging systems, advanced deep learning algorithms, and integrated environmental monitoring has proven highly effective, delivering a precise and reliable incubation process.

Future iterations of the prototype will include an automated removal system for non-viable embryos. This enhancement is expected to prevent the spread of infections, reduce food losses caused by the potential disposal of entire batches, and enable accurate quantification of embryo mortality for better production estimates.

Based on current results and literature data, this system has the potential to increase the percentage of eggs reaching the eyed stage (a more resilient developmental phase) by up to 5%, and in some cases by as much as 20%, thereby improving overall hatchery productivity and sustainability. However, a significant bottleneck remains the immediate scalability and adoption of this technology in commercial aquaculture settings. Most hatcheries currently rely on simpler, cost-effective incubators, and transitioning to a more technologically advanced and expensive system may face resistance due to initial investment requirements and the need for operational adjustments.

4.4.3 Further steps and planning

In the next development phase, the third prototype will undergo further enhancements aimed at increasing its level of automation, precision, and reliability. Planned improvements include: (i) the integration of a slide system designed to efficiently and gently convey embryos from the incubation area to the sorting area, thereby streamlining their handling and exposure to the vision system; and (ii) the development and incorporation of a dedicated selection device capable of automatically removing non-viable or infected embryos based on real-time data provided by the multispectral cameras and deep learning algorithms. Both components are currently in the design and engineering stage, with a focus on ensuring that embryo handling remains safe and non-invasive while maximizing sorting efficiency.

Once these upgrades are completed, the improved third prototype will be re-tested under real farming conditions at the same rainbow trout facility, Società Agricola Troticoltura F.lli Leonardi, in February 2026. This second round of field testing will serve to validate the system's performance in a commercial aquaculture setting, assess its scalability, and gather operational data to further refine its functionality before progressing toward a fully deployable version suitable for large-scale hatchery applications.

Funded by the European Union. Views and opinions expressed are however those of the author(s) only and do not necessarily reflect those of the European Union or the European Research Executive Agency (REA). Neither the European Union nor the granting authority can be held responsible for them.

4.4.4 Policy recommendations

The preliminary achieved results demonstrate that automated systems based on multispectral imaging and deep learning can significantly enhance the early detection and removal of non-viable embryos in aquaculture, thereby reducing production losses. To support the operational deployment of such technologies, policy measures should encourage the development of standardized imaging protocols and performance benchmarks for automated monitoring systems.

Equally important is the establishment of robust data governance frameworks, addressing issues such as data ownership between technology providers and farmers, secure data storage, controlled access, and responsible use of AI-generated insights. Policies should ensure that data collected through automated systems remains transparent, auditable, and compliant with applicable regulations, while protecting commercially sensitive information.

Furthermore, incentives for the adoption of smart aquaculture technologies should be considered, particularly for SMEs, to reduce barriers to entry.

Funded by the European Union. Views and opinions expressed are however those of the author(s) only and do not necessarily reflect those of the European Union or the European Research Executive Agency (REA). Neither the European Union nor the granting authority can be held responsible for them.

5. Blockchain technology implementation in mussel aquaculture

5.1 Overview

The goal of this task is to provide a decentralized digital platform capable of ensuring the non-repudiation and non-alterability of data regarding food loss. Blockchain technology offers an ideal framework for this purpose, as its immutable and distributed nature can serve as the foundation for designing technological solutions that ensure data reliability (Khunaifi et al., 2025, Payandeh et al., 2025). To validate the approach, the proposed platform is applied to certify data collected during the analysis of a case study involving a mussel farm in Senigallia, Marche, Italy.

Timeline (M01–M42):

- M01–M12: Initial architecture set-up of the Blockchain method; Initiation of mussels case
- M13–M24: Building of architecture; data collection mussels
- M25–M42: Implementation of blockchain technology and integration of mussel measurement data

5.2 Materials & Methods

5.2.1 Collected Data

The data acquisition phase in the mussel aquaculture case study focused on collecting biological, environmental, and operational information to be later certified through blockchain technology (Zonneveld et al., 2025). The activities were conducted in collaboration with the *Sena Gallica* cooperative in Senigallia (Italy), where the whole productive cycle of Mediterranean mussel (*Mytilus galloprovincialis*) was monitored during two campaigns (June 2023- May 2024 and June 2024- May 2025).

For each campaign, mussels' socks from 3 sites (named as Small, Medium, and Big according to the size of the mussels' seeds at the beginning of the productive cycle) were sampled over different times of the productive cycle: (i) July (2023 and 2024), November (2023 and 2024), February (2024 and 2025), and May (2024 and 2025, respectively).

At each stage, 3 one-meter samples of mussels' socks were collected to evaluate production losses (mortality rate) and individual parameters (shell length, total wet weight, wet weight of the edible part). During the on-growing phase, mussels were subjected to different natural conditions (seasonal changes, variability of natural climatic conditions and seawater features, and eventual presence of predators). For instance, the presence of polyclad flatworm (*Stylochus mediterraneus*; Turbellaria; a common predator of farmed mussels) was recorded.

Complementary data, including weather and marine conditions, were collected via a buoy managed by the Italian National Research Council (CNR). To enhance precision, a prototype IoT system was designed for monitoring mussel growth (in terms of whole sock), while the

Funded by the European Union. Views and opinions expressed are however those of the author(s) only and do not necessarily reflect those of the European Union or the European Research Executive Agency (REA). Neither the European Union nor the granting authority can be held responsible for them.

blockchain platform was designed to guarantee the traceability and integrity of all collected data.

The harvest for local distribution occurred in May 2024 and 2025 and involved mussels at market size. At this stage, 9 socks were subjected to the cleaning procedure through the automatic machine (company: Cocci Luciano srl) that removed the plastic nets and the mud and then progressively separated, according to their size: (i) cleaned mussels ready to be sold; (ii) mussel seeds; (iii) dead mussels under market size; (iv) dead mussels at market size. The percentage incidence of each category (based on their total weight) was calculated, also considering the cleaned mussels that were only slightly damaged by the cleaning procedure and those completely broken (food loss).

An additional data acquisition campaign related was undertaken related to the cold chain. The temperature of a batch of mussels shipped from Senigallia to Siracusa, IT was also monitored. One of the main objectives was to evaluate the dynamics of temperature during the trip. High temperatures represent an issue for quality and safety. A dataset of 6000+ datapoints was recorded at the end of Feb'25 using a dedicated data-logger (i.e. Elitech RC-5+). No anomalies in terms of temperature variation have been detected during the shipment (which lasted approximatively 17 hours), confirming the maintenance of proper transport conditions for mussels.

5.2.2 Brief overview of processing

Prior to certification, the datasets were cleaned to remove outliers, and descriptive statistics (mean values and standard deviations) were computed to prepare them for further analysis.

Overall, this data acquisition strategy ensured comprehensive monitoring of the production cycle, capturing biological performance, environmental variables, and food loss factors, while providing a secure digital framework for data validation and transparency.

5.2.3 Method development activities

A blockchain-based system is developed to certify and secure data in mussel aquaculture. The method uses an off-chain server to gather inputs from web, mobile, and IoT sources, while cryptographic proofs are stored on a public blockchain. Through mechanisms like Merkle trees, the approach ensures data integrity, traceability, and cost-efficient certification without exposing sensitive information.

5.3 First Results

5.3.1 General workflow

Prerequisites

Firstly, the *Super Admin* must create a new supply chain and define a supply chain identifier, a name and an eventual description. Then, if not already present, the *Super Admin* must insert a new data owner into the platform. Some information is required for creation, such as the owner's name, a description, a logo and eventual contacts (address, email, telephone, etc).

Funded by the European Union. Views and opinions expressed are however those of the author(s) only and do not necessarily reflect those of the European Union or the European Research Executive Agency (REA). Neither the European Union nor the granting authority can be held responsible for them.

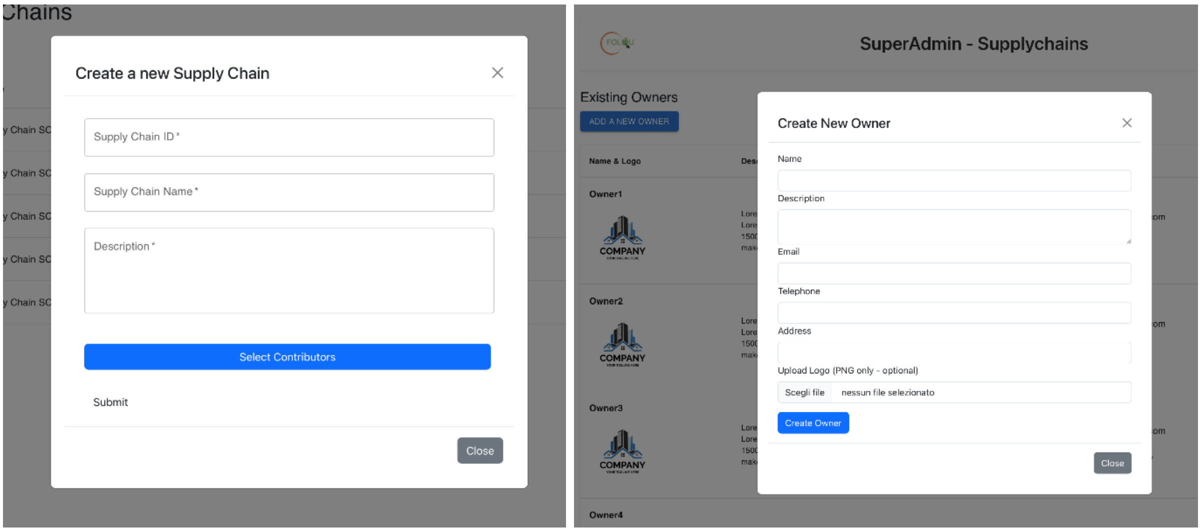

Figure 5.1 Creation of the supply chain (left) and of the owner (right).

Next, a new *Staff* or *Local Admin* user must be created for the owner. The user is defined by an email, a temporary password (the user will have to change it), the role type and the related owner.

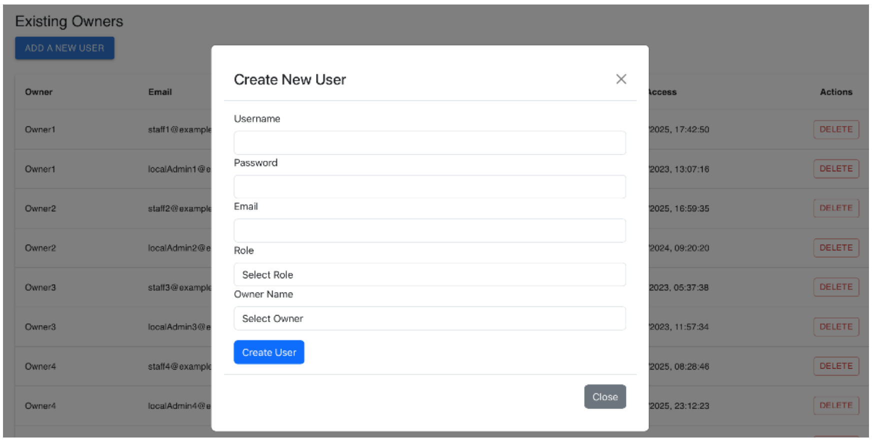

Figure 5.2 New user creation

<u>Data upload and certification</u>

Staff users can upload new data by filling out a form. This form can be customized to include arbitrary data fields with a name and a value. These data must be associated with an existing supply chain so that it is correctly retrieved when the supply chain is explored. The uploaded data are then permanently stored in an off-chain database.

Funded by the European Union. Views and opinions expressed are however those of the author(s) only and do not necessarily reflect those of the European Union or the European Research Executive Agency (REA). Neither the European Union nor the granting authority can be held responsible for them.

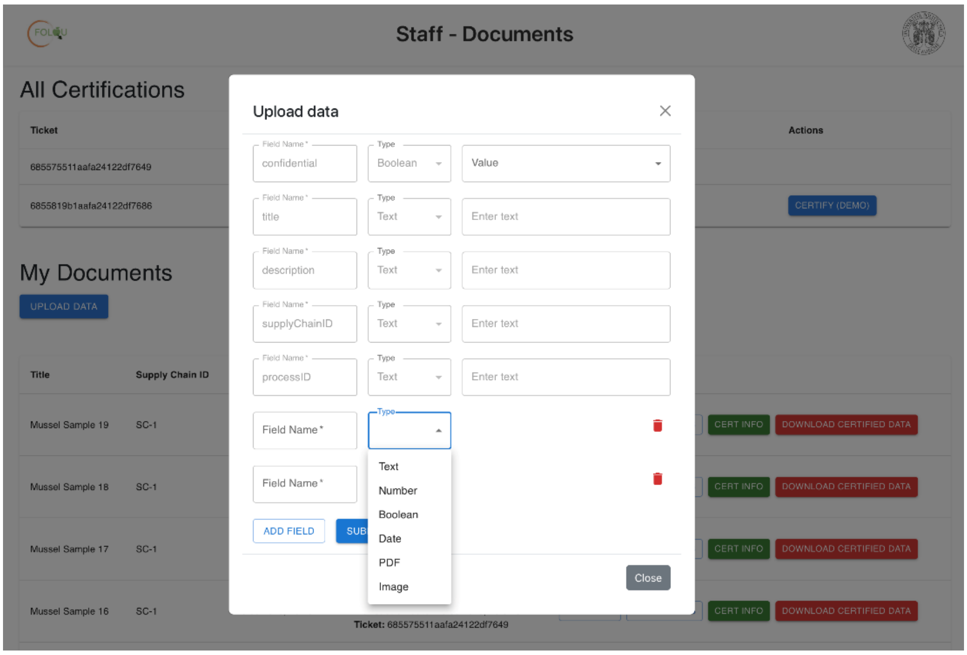

Figure 5.3 Data uploading

The *Staff user* can perform various operations on these data: deletion, certification request or abortion and integrity proof download. Data can be deleted until a certification request has not been submitted. The certification is automatically made by the application upon user request and confirmation. While the data undergo formatting validation, the accuracy and truthfulness of the provided information are the sole responsibility of the data submitter. Before the data are effectively certified, it is possible to abort the certification request. Once the data have been certified, the only permitted operation is to download the data together with the blockchain-based proof of integrity. This is useful if the data owner decides to share a particular piece of data. This operation is not necessary if the certification verification is carried out by exploring the supply chain. Indeed, it is possible to directly use the platform itself to track all the data related to a specific supply chain. The certification lifecycle can be tracked by the *Staff user* by monitoring the status of the certification procedure of the data. Admitted status are reported in the following table:

Status	**Description**
Not certified	The certification has not been requested yet.
Pending	The certification request has been submitted and is being processed.
Failed	The certification process failed for some reasons.
Completed. Certification to be downloaded	The certification was successful, certification information is ready to be attached to the related data.
Completed	The certification information has been downloaded and the certification procedure is finalized.

Funded by the European Union. Views and opinions expressed are however those of the author(s) only and do not necessarily reflect those of the European Union or the European Research Executive Agency (REA). Neither the European Union nor the granting authority can be held responsible for them.

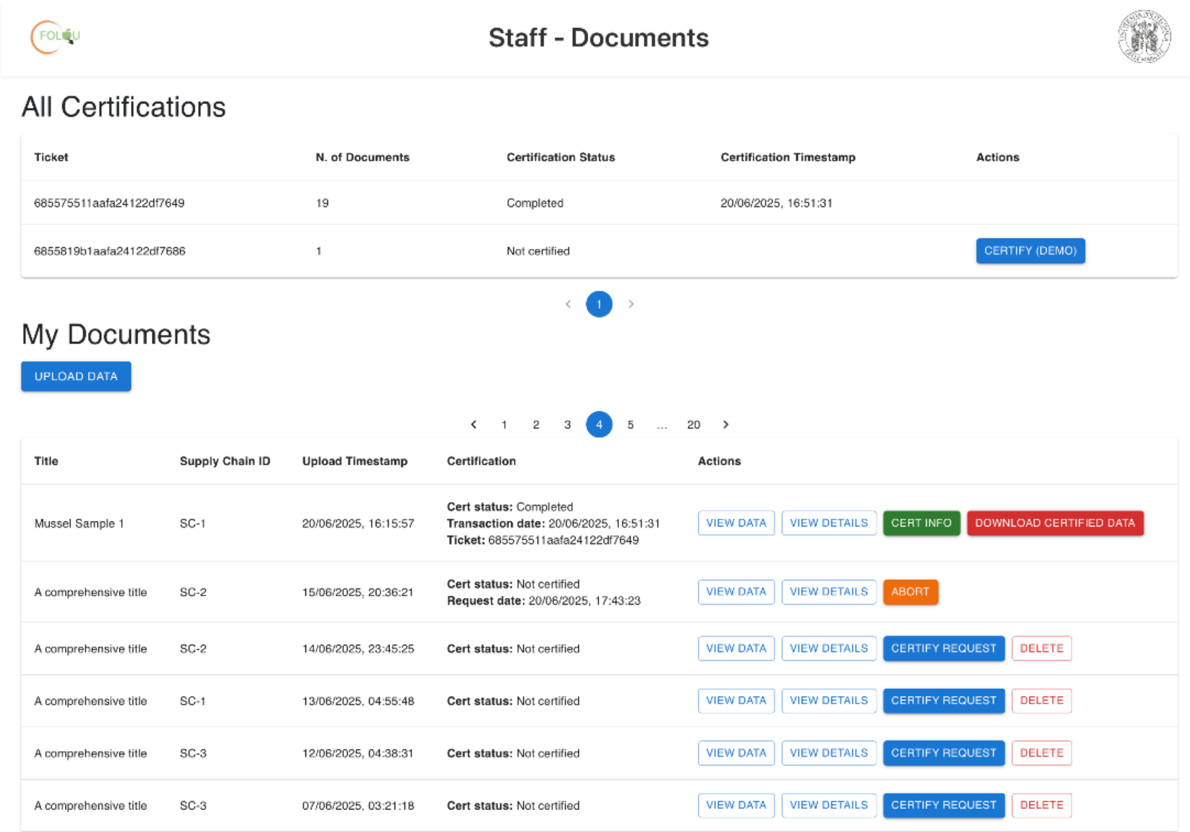

Figure 5.4 Dashboard with all documents that are certified or waiting to be certified. The certification and verification procedures are those detailed in the deliverable D3.1.

<u>Supply chain exploration and data certification verification</u>

Guest users may be interested in exploring a supply chain and reading all the published data alongside their certification proof. To do this, a specific section of the platform allows to search for all the data of a given supply chain. While searching, it is possible apply filters such as start and end date of data upload, data owners, only certified data. Once the desired data have been found, the published data can be read and their certification proof verified (i.e., whether integrity has been verified, the blockchain name and transaction hash, time of the certification). If a *Staff user* has shared certified data outside the platform, a *Guest user* can upload them and verify their validity.

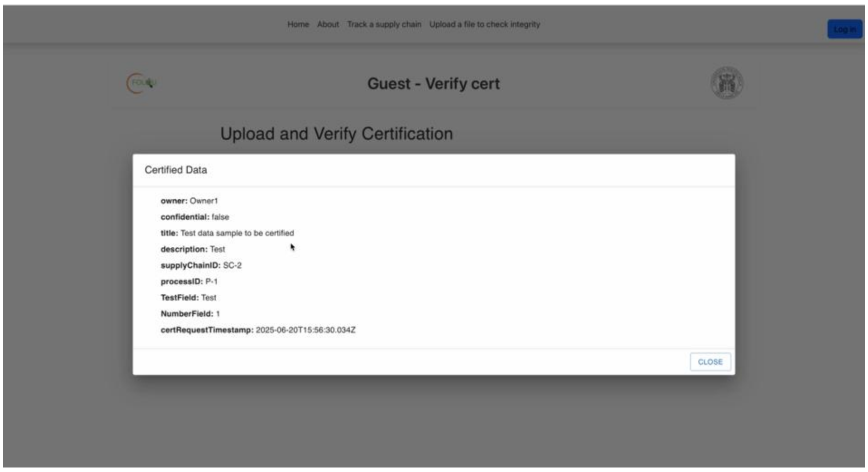

Figure 5.5 Procedure for the verification of the certified data

Funded by the European Union. Views and opinions expressed are however those of the author(s) only and do not necessarily reflect those of the European Union or the European Research Executive Agency (REA). Neither the European Union nor the granting authority can be held responsible for them.

5.3.2 Security aspects

The platform integrates multiple security layers:

- **Session Cookies** for secure user sessions
- **Change password** for *Staff*, *Local Admin* and *Super Admin* accounts
- **Two-Factor Authentication** (2FA) for *Staff*, *Local Admin* and *Super Admin* accounts
- **Blockchain-based certification**

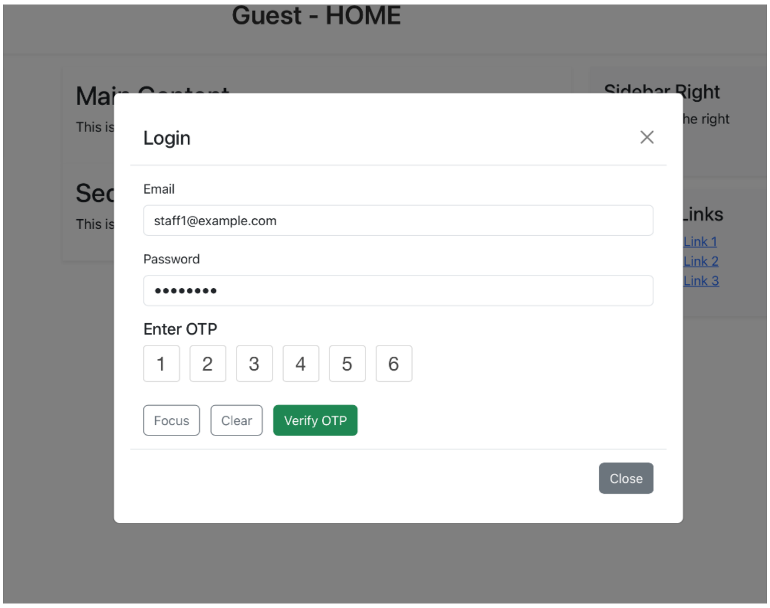

Figure 5.6 Two-factor authentication

5.3.3 Test with real data

The platform has been tested using the mussels data collected as described in Section 5.2.1. Using the application, indeed, it is possible to store collected data in a reliable, secure, and immutable way. Moreover, a *Guest user* can monitor all the information related to the specific supply chain simply using the platform itself, as shown in the figure below.

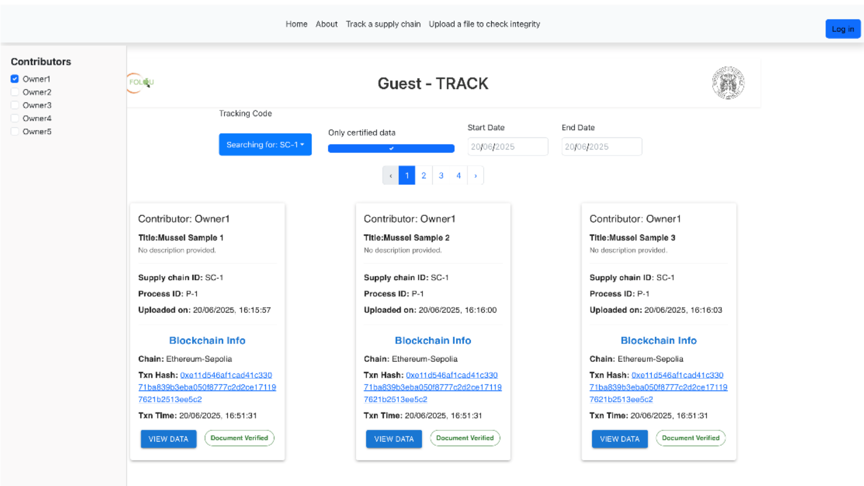

Figure 5.7 Results of the certification testing of mussels related data

Funded by the European Union. Views and opinions expressed are however those of the author(s) only and do not necessarily reflect those of the European Union or the European Research Executive Agency (REA). Neither the European Union nor the granting authority can be held responsible for them.

Furthermore, the platform has been used to store, among the others, data related to food loss. Specifically, by exploring data from the mussel supply chain, the amount (weight) of dead mussels at market size and the amount (weight) of mussels irreparably damaged during the cleaning process were identified as the key two parameters determining production losses. Both can be retrieved with the blockchain method.

5.4 Discussion

5.4.1 Results vs original goal

The activities progressed in line with the original objectives, and the planned results were successfully achieved. The developed solutions performed as expected, with no major deviations from the initial goals.

5.4.2 Key successes and bottlenecks

The development of the blockchain-based application has reached a solid level of maturity, with the core functionalities already operational. A significant success has been the start of real data certification: as described in Section 5.3.3, the first datasets related to mussel production have been securely recorded, demonstrating the feasibility and reliability of the proposed approach. This marks an important step towards achieving full traceability and transparency within the aquaculture value chain.

In terms of bottlenecks, the overall process has not encountered substantial technical or organizational barriers. However, one aspect that may become critical soon is the transition from the current test environment to the Ethereum mainnet. While this step is necessary to ensure full-scale deployment and public verifiability, it implies transaction costs that could affect the economic sustainability of continuous certification. Careful evaluation of cost-efficiency strategies will therefore be important in the next stages of development.

5.4.3 Further steps and planning

At present, the application is running locally, and the next step is to deploy it online. This will not only make the system more widely accessible but also increase the number of people able to test it and provide valuable feedback

Beyond this, the team is exploring ways to extend the platform functionalities by integrating food loss certification. A first formula has already been developed to calculate food loss related to mussel harvesting, and this metric will be incorporated into the application. One promising option under consideration is the use of a smart contract, which would allow for automated and transparent certification of food loss data directly on the blockchain. These enhancements will strengthen the platform role as a comprehensive tool for ensuring traceability, integrity, and sustainability in mussel aquaculture extending other existing approaches (Capoccioni et al., 2023).

Funded by the European Union. Views and opinions expressed are however those of the author(s) only and do not necessarily reflect those of the European Union or the European Research Executive Agency (REA). Neither the European Union nor the granting authority can be held responsible for them.

5.4.4 Policy recommendations

The initial obtained results confirm that blockchain-based platforms can provide a reliable mechanism to ensure the integrity, transparency, and traceability of data related to food losses (Compagnucci et al., 2022). To enable large-scale adoption, policy frameworks should support the definition of common standards for data certification, interoperability, and governance across stakeholders in the agri-food supply chain also promoting the use of European infrastructures that could be shared across multiple projects.

In this context, data governance is a key element, requiring clear rules on data ownership, permissioned access, and responsibilities across distributed systems. Policies should address how data is validated before being recorded on-chain, how off-chain data is managed, and how accountability is maintained in decentralized environments. Particular attention should be given to balancing transparency with privacy, including compliance with data protection regulations and protection of sensitive business information.

Public support for pilot projects and real-world implementations, such as the mussel farming case study with cold chain related aspects, can help demonstrate feasibility and build trust among stakeholders.

Funded by the European Union. Views and opinions expressed are however those of the author(s) only and do not necessarily reflect those of the European Union or the European Research Executive Agency (REA). Neither the European Union nor the granting authority can be held responsible for them.

6. Market demand tools from social networks (T3.6, CIRCE)

6.1 Introduction

The objective of the task is to increase the accuracy in the estimation of food consumption, by exploiting information of online trends. With this purpose, CIRCE applied natural language processing and machine learning to predict food consumption in five commodities, based on queries to a search engine and posts from a social network. In this period, additional data was collected for search interest and food consumption, consumption models were trained and validated with part of the query dataset, and sentiment analysis was applied to social network posts.

Timeline (M01–M42):

- M07–M24: Initial outline, identification of the social media and network (X, Google search) to be analysed, data retrieval, initial analysis of network (Google search) data
- M25–M42: Full method development for network (Google search) and social media data

6.2 Materials & methods

6.2.1 Collected data

The dataset of search interest and food consumption was expanded with monthly samples from 2004 to 2017. The number of samples was tripled, for a total of 240 monthly samples. The acquisition procedure of D3.1 was followed.

6.2.2 Brief overview of processing

Network posts required processing. They were not catalogued or pertained to any specific language, country, or theme, and therefore had to be classified into relevant categories in order to filter out all irrelevant posts. The first step consisted of language labelling. Spanish posts were kept to study the use case of the project.

The next step was the lemmatization of the corpus, i.e. dataset of posts. A lemma is the base or dictionary form of a word (e.g., *run* for *running, ran, runs*), and lemmatization is the process of reducing words to their lemma using vocabulary and grammar rules. Once every post was lemmatized, list comparison was conducted in order to retain posts that contained one or more words related to five foods under study: tomato, olive oil, hake, pasta and pork.

Once the corpus was fully lemmatized, a sentiment analysis process was conducted, labelling each post into one of five sentiment categories: anger, joy, surprise, sadness, and fear. For sentiment analysis, a BERT-based pre-trained model was used. In short, BERT is a transformer-based model trained with masked language modelling and next-sentence prediction to capture bidirectional context. RoBERTa improves on BERT by removing next-sentence prediction, training on much more data, and using dynamic masking for better

Funded by the European Union. Views and opinions expressed are however those of the author(s) only and do not necessarily reflect those of the European Union or the European Research Executive Agency (REA). Neither the European Union nor the granting authority can be held responsible for them.

performance. A RoBERTa model for the Spanish language was used[2], providing a score for each sentiment. The emotion with the highest scoring was assigned as label. The number of posts was computed for each food, sentiment, and month. The result was divided by the total number of monthly posts for that food, returning a sentiment ratio. A corpus of 400 GB was processed, comprising the period between January and September 2018.

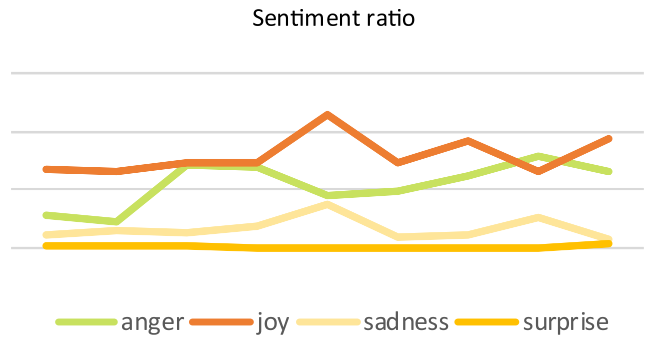

Figure 6.1 Evolution of monthly sentiment ratio, example results for hake

Network posts reflected a different tendency for each food and sentiment. Hake had a higher proportion of joy-labelled posts. Joy and anger were the predominant sentiments for olive oil. Pork, pasta, and tomato were mainly associated to anger emotion. The first two cases were affected by polysemy in Spanish, associated to colloquial expressions for insult and money.

6.2.3 Method development activities

Models of food consumption based on search queries were trained and validated. This activity employed 80 % of data, from 2004 to 2018. The model variables (prediction targets and input features) are defined in Table 6.1. The linear relationship of consumption with price and search interest was characterized with the Pearson correlation coefficient (PCC).

Table 6.1. Prediction targets and input features defined for the modelling of search queries

Variable type	Feature name	Notes
Prediction target	Consumption one month ahead, c_{k+1}	-
	Consumption four months ahead, c_{k+4}	-
	Consumption seven months ahead, c_{k+7}	-
	Consumption ten months ahead, c_{k+10}	-
Input features	Consumption four months ago, c_{k-4}	-
	Consumption five months ago, c_{k-5}	-
	Consumption eight months ago, c_{k-8}	-
	Consumption eleven months ago, c_{k-11}	-
	Price four months ago, p_{k-4}	-

[2] https://huggingface.co/daveni/twitter-xlm-roberta-emoti-on-es

Funded by the European Union. Views and opinions expressed are however those of the author(s) only and do not necessarily reflect those of the European Union or the European Research Executive Agency (REA). Neither the European Union nor the granting authority can be held responsible for them.

	Search interest one month ago, i_{k-1}	Extracted from search engine
	Current date, t	Examples: • 2017.00 (January 2017) • 2017.08 (February 2017) • 2017.92 (December 2017) • 2018.00 (January 2018)

The effect of search interest on the prediction of consumption was evaluated with a set of nine models per forecast horizon and food (Table 6.2). Search interest was included as input feature in three models, and the remaining models were used as baseline. The models employed algorithms of exponential smoothing (ES), linear regression (LR), support vector machines (SVM), and multilayer perceptron (MLP). Most models used at least one input feature from Table 6.1.

Two models employed additional input features, described in more detail in Table 6.2. Different hyperparameters were evaluated for the algorithms. A cross-validation with rolling forecasting origin and five folds was applied. The models were evaluated with the mean absolute error (MAE). The error was divided by the average consumption of each product to compare results between commodities.

Table 6.2. Effect of search interest on the prediction of consumption: models evaluated for every forecast horizon and food.

Model type	Model ID	Algorithm	Input features	Tuning of hyperparameters
Baseline, search interest is not used as input feature	1	Exponential smoothing	Historical consumption, from 2004 to four months before prediction	Trend (regular, damped)
	2	Linear regression	c_{k-4}	-
	3		Consumption twelve months before forecast horizon	-
	4		c_{k-4}, c_{k-5}, c_{k-8}, c_{k-11}, p_{k-4}, t	-
	5	Support vector machines		Regularization term (10^{-2},10^{0},10^{2})
	6	Multilayer perceptron		Neuron layers (10, 7/5/3, 50/30/10), regularization term (10^{-6}, 10^{-4}, 10^{-2})
Novel, search interest is used as input feature	7	Linear regression	c_{k-4}, c_{k-5}, c_{k-8}, c_{k-11}, p_{k-4}, i_{k-1}, t	-
	8	Support vector machines		Regularization term (10^{-2},10^{0},10^{2})
	9	Multilayer perceptron		Neuron layers (10, 7/5/3, 50/30/10), regularization term (10^{-6}, 10^{-4}, 10^{-2})

Funded by the European Union. Views and opinions expressed are however those of the author(s) only and do not necessarily reflect those of the European Union or the European Research Executive Agency (REA). Neither the European Union nor the granting authority can be held responsible for them.

Food consumption for a specific month was also modelled based on network posts of the same month. Two types of linear regression were evaluated: univariate and multivariate. A univariate model was defined for each food and sentiment, using as input sentiment ratio. An additional univariate model was studied for each food, employing the number of posts associated to each food, without introducing sentiment information. Multivariate models were built for each commodity using the five sentiment ratios as features. All the post models were evaluated based on R^2.

6.3 First results

Search interest had a moderate linear relationship with consumption (|PCC|=0.55) for pasta, olive oil, and hake. The correlation for tomato and pork was weaker (|PCC|<0.20). During the training of the query models, the use of search interest with the MLP algorithm provided the lowest error (MAE<4 %) for 55 % of the cases. In the remaining scenarios, ES and MLP without search interest had a higher accuracy (MAE<6 %). Depending on model selection, the MAE changed 4 % on average.

The performance of models with search interest decreased during validation, reaching the lowest error (MAE<10 %) for 10 % of the cases. ES and LR were the best algorithms in 90 % of the scenarios (MAE<12 %). MAE was reduced 4 % due to model selection, reproducing its behaviour during training. Figure 6.1 shows the minimum MAE measured for each food and forecast horizon.

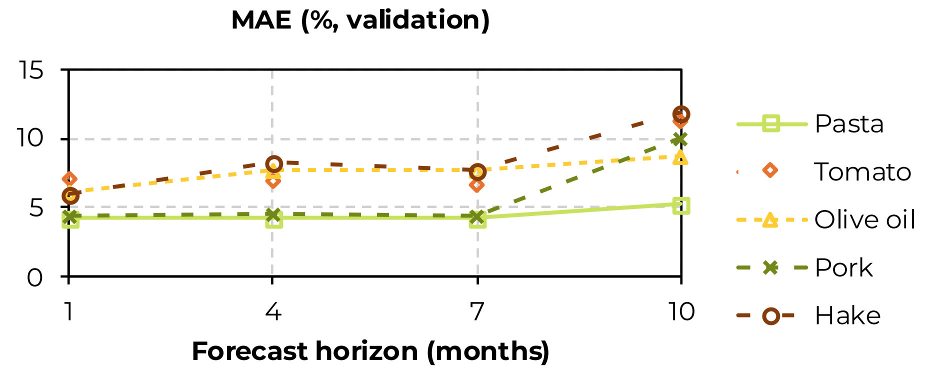

Figure 6.1 Minimum MAE (%) achieved during model validation for each food and forecast horizon

Univariate models based on sentiment ratio and post number had a weak correlation in general ($R^2 < 0.7$, Figure 6.2). These results were improved with multivariate models ($0.4 < R^2 < 1.0$, Figure 6.3). Pork and hake presented a lower correlation between food consumption and sentiment ratio ($0.4 < R^2 < 0.8$). A finer adjustment was exhibited for pasta, tomato, and olive oil ($0.8 < R^2 < 1.0$).

Funded by the European Union. Views and opinions expressed are however those of the author(s) only and do not necessarily reflect those of the European Union or the European Research Executive Agency (REA). Neither the European Union nor the granting authority can be held responsible for them.

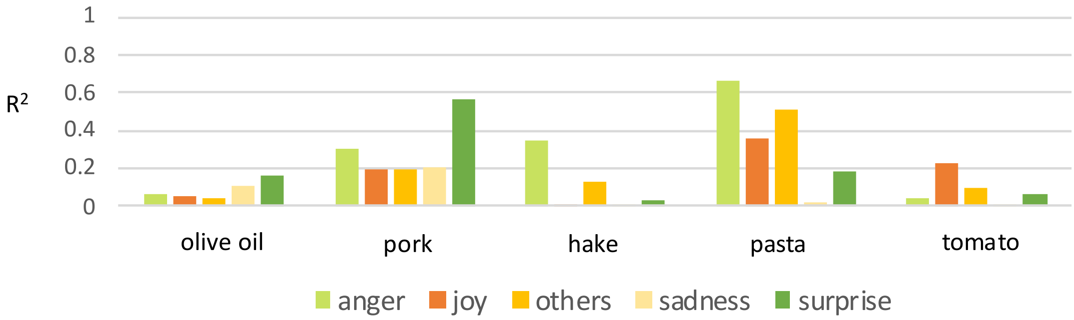

Figure 6.2. R2 of univariate regression with sentiment ratio

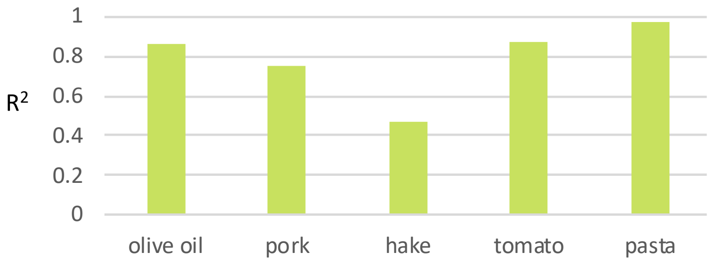

Figure 6.3. R2 of multivariate regression with sentiment ratio

6.4 Discussion

6.4.1 Results vs original goal

An initial assessment of model accuracy was performed in the estimation of food consumption. The forecasts can be compared with supply information to quantify food loss in surplus scenarios. CIRCE activities show that search queries can improve model performance, and posts from social networks can describe consumption variations. These alternatives have exhibited their application potential for the food sector.

6.4.2 Key successes and bottlenecks

The search interest was correlated with the future consumption of three out of five food cases. The integration of search interest as model input increased the estimation accuracy in most training cases, and in some validation scenarios. Data sources with weekly or daily granularity could increase the modelling potential with higher data volumes. The development of models for shorter time periods could enhance their adjustment to changes in variable correlations.

The proposed processing for posts was validated as an efficient alternative for filtering and sentiment analysis. Despite the significant size of the initial corpus (400 GB), the evaluation of additional posts could still increase the generalization of the results. The correlation between food consumption and post sentiments could be enhanced with topic and spatial classification.

Funded by the European Union. Views and opinions expressed are however those of the author(s) only and do not necessarily reflect those of the European Union or the European Research Executive Agency (REA). Neither the European Union nor the granting authority can be held responsible for them.

6.4.3 Further steps and planning

Query models will be tested for data between 2018 and 2023, without receiving further training in the process. Press releases of the Spanish Ministry of Agriculture, Fisheries and Food will be employed to give additional context in this period. Furthermore, additional posts will be acquired and processed.

6.4.4 Policy recommendations

Food demand can be predicted reliably with historical consumption data; Adding internet search or social media can improve these models further. Such models can be instrumental in anticipating to food demand and avoiding future food losses.

Funded by the European Union. Views and opinions expressed are however those of the author(s) only and do not necessarily reflect those of the European Union or the European Research Executive Agency (REA). Neither the European Union nor the granting authority can be held responsible for them.

Conclusion

The present document reports the progress updates of all WP3 tasks while presenting the first initial results of the methods defined and developed in D3.1. The outputs confirm the feasibility and the potential of the proposed approaches across the different commodities addressed in FOLOU.

These initial test results provide a solid base and support for upcoming maturity, optimization and validation steps and the development of advanced features to enhance the performance and applicability of each innovation.

As a conclusion, the work accomplished offers a starting point for validation with manual quantification activities under WP4 and the replication planned within the Twinning Regions Programme (WP7).

Funded by the European Union. Views and opinions expressed are however those of the author(s) only and do not necessarily reflect those of the European Union or the European Research Executive Agency (REA). Neither the European Union nor the granting authority can be held responsible for them.

References

Blanc, L., Lampurlanés, J., Simon-Miquel, G., Jean-Marius, L., & Plaza-Bonilla, D. (2024). Rapeseed-pea intercrop outperforms wheat-legume ones in land-use efficiency in Mediterranean conditions. *Field Crops Research*, 318, 109612. https://doi.org/10.1016/j.fcr.2024.109612

Capoccioni, F., Bille, L., Colombo, F., Contiero, L., Martini, A., Mattia, C., Napolitano, R., Tonachella, N., Toson, M., & Pulcini, D. (2023). A predictive model for the bioaccumulation of okadaic acid in *Mytilus galloprovincialis* farmed in the northern Adriatic Sea: A tool to reduce product losses and improve mussel farming sustainability. *Sustainability, 15*(11), 8608. https://doi.org/10.3390/su15118608

Cardona, E., Bugeon, J., Segret, E., & Bobe, J. (2020). VisEgg: a robust phenotyping tool to assess rainbow trout egg features and viability. *Fish Physiology and Biochemistry*, 47(3), 671–679. https://doi.org/10.1007/s10695-020-00844-2

Celesti, M., van der Tol, C., Cogliati, S., Panigada, C., Yang, P., Pinto, F., Rascher, U., Miglietta, F., Colombo, R., & Rossini, M. (2018). Exploring the physiological information of sun-induced chlorophyll fluorescence through radiative transfer model inversion. *Remote Sensing of Environment, 215*, 97–108. https://doi.org/10.1016/j.rse.2018.05.013

Compagnucci, L., Lepore, D., Spigarelli, F., Frontoni, E., Baldi, M., & Di Berardino, L. (2022). Uncovering the potential of blockchain in the agri-food supply chain: An interdisciplinary case study. *Journal of Engineering and Technology Management, 65*, 101700. https://doi.org/10.1016/j.jengtecman.2022.101700

Duan, S.-B., Li, Z.-L., Wu, H., Tang, B.-H., Ma, L., Zhao, E., & Li, C. (2014). Inversion of the PROSAIL model to estimate leaf area index of maize, potato, and sunflower fields from unmanned aerial vehicle hyperspectral data. *International Journal of Applied Earth Observation and Geoinformation, 26*, 12–20. https://doi.org/10.1016/j.jag.2013.05.007

Hu, J., Fan, C., Wang, Z. & Wu, S. (2023) Fruit Detection and Counting in Apple Orchards Based on Improved Yolov7 and Multi-Object Tracking Methods. *Sensors* 23(13): 5903. https://doi.org/10.3390/s23135903

Kang H. & Chen C. (2020) Fast implementation of real-time fruit detection in apple orchards using deep learning. *Computers and Electronics in Agriculture*, 168: 105108 https://doi.org/10.1016/j.compag.2019.105108

Khunaifi, A., Handoyo, K. M., Wijananto, F., Santoso, T. M., Sahreza, Y., Juliansyah, M. R., Syariati, A. R., Rafianti, D. S., Prasetiyo, A. P., & Harmanda, T. T. (2025). Technical benefits of ISPO certification in blockchain-based supply chain management: A systematic literature review with statistical analysis. In *2025 International Conference on Artificial Intelligence and Technological Solutions (ICAITech)* (pp. 370–375). IEEE. https://doi.org/10.1109/ICAITech66481.2025.11387644

Koirala, A., Walsh, K.B., Wang, Z., McCarthy, C. (2019) Deep learning – Method overview and review of use for fruit detection and yield estimation. Computers and Electronics in Agriculture, 162: 219-234. https://doi.org/10.1016/j.compag.2019.04.017

Li, W., Weiss, M., Garric, B., Champolivier, L., Jiang, J., Wu, W., & Baret, F. (2023). Mapping crop leaf area index and canopy chlorophyll content using UAV multispectral imagery: Impacts of illuminations and distribution of input variables. *Remote Sensing, 15*(6), 1539. https://doi.org/10.3390/rs15061539

Funded by the European Union. Views and opinions expressed are however those of the author(s) only and do not necessarily reflect those of the European Union or the European Research Executive Agency (REA). Neither the European Union nor the granting authority can be held responsible for them.

Lindholm-Lehto, P. C., & Pylkkö, P. (2024). Saprolegniosis in aquaculture and how to control it? *Aquaculture, Fish and Fisheries, 4*(4). https://doi.org/10.1002/aff2.200

Longmire, A. R., Poblete, T., Hunt, J. R., Chen, D., & Zarco-Tejada, P. J. (2022). Assessment of crop traits retrieved from airborne hyperspectral and thermal remote sensing imagery to predict wheat grain protein content. *ISPRS Journal of Photogrammetry and Remote Sensing, 193*, 284–298. https://doi.org/10.1016/j.isprsjprs.2022.09.015

Payandeh, R., Delbari, A., Fardad, F., Helmzadeh, J., Shafiee, S., & Ghatari, A. R. (2025). Unraveling the potential of blockchain technology in enhancing supply chain traceability: A systematic literature review and modeling with ISM. *Blockchain: Research and Applications, 6*(1), 100240. https://doi.org/10.1016/j.bcra.2024.100240

Prikaziuk, E., Ntakos, G., ten Den, T., Reidsma, P., van der Wal, T., & van der Tol, C. (2022). Using the SCOPE model for potato growth, productivity and yield monitoring under different levels of nitrogen fertilization. *International Journal of Applied Earth Observation and Geoinformation, 114*, 102997. https://doi.org/10.1016/j.jag.2022.102997

Rivosecchi, C., Mancini, A., Mammarella, F., Cuscianna, A., Deligios, P. A., Fattorini, M., Fiorentini, M., Francioni, M., Bianchini, M., & Ledda, L. (2024). Evaluating the impact of various agronomic management practices on food loss at the primary production stage using proximal and remote sensing. In *2024 IEEE International Workshop on Metrology for Agriculture and Forestry (MetroAgriFor)* (pp. 643–648). IEEE. https://doi.org/10.1109/MetroAgriFor63043.2024.10948777

Rohani, A., Taki, M., & Bahrami, G. (2019). Application of artificial intelligence for separation of live and dead rainbow trout fish eggs. *Artificial Intelligence in Agriculture, 1*, 27–34. https://doi.org/10.1016/j.aiia.2019.03.002

van der Tol, C., Verhoef, W., Timmermans, J., Verhoef, A., & Su, Z. (2009). An integrated model of soil-canopy spectral radiances, photosynthesis, fluorescence, temperature and energy balance. *Biogeosciences, 6*(12), 3109–3129. https://doi.org/10.5194/bg-6-3109-2009

Wang, A., Chen, H., Liu, L., Chen, K., Lin, Z., & Han, J. (2024). Yolov10: Real-time end-to-end object detection. *Advances in Neural Information Processing Systems*, *37*, 107984-108011. https://arxiv.org/abs/2405.14458

Webber, H., Zhao, G., Wolf, J., Britz, W., de Vries, W., Gaiser, T., Hoffmann, H., & Ewert, F. (2015). Climate change impacts on European crop yields: Do we need to consider nitrogen limitation? *European Journal of Agronomy*, 71, 123–134. https://doi.org/10.1016/j.eja.2015.09.002

Weiss, M., Baret, F., Myneni, R. B., Pragnère, A., & Knyazikhin, Y. (2000). Investigation of a model inversion technique to estimate canopy biophysical variables from spectral and directional reflectance data. *Agronomie, 20*(1), 3–22. https://doi.org/10.1051/agro:2000105

Zhu, X., Skidmore, A. K., Darvishzadeh, R., & Wang, T. (2019). Estimation of forest leaf water content through inversion of a radiative transfer model from LiDAR and hyperspectral data. *International Journal of Applied Earth Observation and Geoinformation*, 74, 120–129. https://doi.org/10.1016/j.jag.2018.09.008

Zonneveld, G., Rafaiani, G., Battaglioni, M., & Baldi, M. (2025). Data certification strategies for blockchain-based traceability systems. In *2025 IEEE International Conference on Blockchain and Cryptocurrency (ICBC)* (pp. 1–8). IEEE. https://doi.org/10.1109/ICBC64466.2025.11114484

Funded by the European Union. Views and opinions expressed are however those of the author(s) only and do not necessarily reflect those of the European Union or the European Research Executive Agency (REA). Neither the European Union nor the granting authority can be held responsible for them.